energies

MDPI

*Review*

# A Review on $CO_2$ Sequestration via Mineralization of Coal Fly Ash

**Long Jiang [1], Liang Cheng [1], Yuxuan Zhang [2], Gaojun Liu [1] and Jian Sun [2,*]**

[1] North China Electric Power Research Institute Co., Ltd., Beijing 100045, China; kaveykikiy@163.com (L.J.); chengliang@ncepri.com.cn (L.C.); liu.gao.jun@163.com (G.L.)
[2] School of Energy and Mechanical Engineering, Nanjing Normal University, Nanjing 210042, China; 221912019@njnu.edu.cn
* Correspondence: jiansun@njnu.edu.cn

**Abstract:** Coal fly ashes (COFA) are readily available and reactive materials suitable for $CO_2$ sequestration due to their substantial alkali components. Therefore, the onsite collaborative technology of COFA disposal and $CO_2$ sequestration in coal-fired power plants appears to have potential. This work provides an overview of the state-of-the-art research studies in the literature on $CO_2$ sequestration via the mineralization of COFA. The various $CO_2$ sequestration routes of COFA are summarized, mainly including direct and indirect wet carbonation, the synthesis of porous $CO_2$ adsorbents derived from COFA, and the development of COFA-derived inert supports for gas-solid adsorbents. The direct and indirect wet carbonation of COFA is the most concerned research technology route, which can obtain valued Ca-based by-products while achieving $CO_2$ sequestration. Moreover, the Al and Si components rich in fly ash can be adapted to produce zeolite, hierarchical porous nano-silica, and nano-silicon/aluminum aerogels for producing highly efficient $CO_2$ adsorbents. The prospects of $CO_2$ sequestration technologies using COFA are also discussed. The objective of this work is to help researchers from academia and industry keep abreast of the latest progress in the study of $CO_2$ sequestration by COFA.

**Keywords:** coal fly ash; mineralization; $CO_2$ sequestration; direct and indirect carbonation



**Citation:** Jiang, L.; Cheng, L.; Zhang, Y.; Liu, G.; Sun, J. A Review on $CO_2$ Sequestration via Mineralization of Coal Fly Ash. *Energies* **2023**, *16*, 6241. https://doi.org/10.3390/en16176241

Academic Editor: Sohrab Zendehboudi

Received: 11 July 2023
Revised: 24 July 2023
Accepted: 28 July 2023
Published: 28 August 2023



## 1. Introduction

COFA is a type of solid waste from power plants derived from the combustion of coal [1]. Every year, a large amount of COFA is generated as the demand for cheap electricity increases [2]. As the world's largest consumer of coal, nearly 80% of coal is consumed to produce electricity each year in China [3], producing 827 million tons of COFA in 2022. Although partial COFA is used as supplementary feedstocks to make roadbed and water-permeable bricks or as the raw materials to synthesize zeolite [4], a good deal of COFA is still accumulated or disposed of in landfills, causing harmful impacts on the local environment [5]. In addition, because heat power plants are also major sources of $CO_2$ emissions, it is urgent to achieve $CO_2$ reduction in coal-fired power plants via $CO_2$ capture and storage technologies [6,7]. COFAes are inexpensive, convenient, and reactive materials suitable for mineral carbonation due to their substantial alkali and alkali earth metals [1,8]. Therefore, the onsite collaborative treatment of COFA disposal and $CO_2$ sequestration in heat power plants can gain significant advantages [2,9]. It is similar to $CO_2$ storage by enhanced oil recovery (EOR) and enhanced gas recovery (EGR) technologies [10–12], which provide additional benefits while achieving $CO_2$ sequestration.

Generally, mineral $CO_2$ sequestration using COFA is mainly classified into two types, including direct and indirect carbonation. Typically, direct carbonation of COFA can be accomplished by aqueous mineral carbonation or gas-solid reactions. Indirect carbonation contains the extraction of $Ca^{2+}$ and $Mg^{2+}$ from COFA by leaching agents (i.e., acid, ammonium salt, etc.) followed by carbonation reactions [13]. While sequestering $CO_2$, the final

carbonated products of COFA via direct carbonation can be used as construction fillers because their physical structure and leaching resistance are enhanced as well. The indirect carbonation of COFA allows for the production of pure carbonates due to the removal of impurities (i.e., silica and iron) prior to carbonate precipitation. Hence, these can enhance the economy of the carbonation treatment while decreasing the overall environmental influence of COFA. Moreover, COFA can also be used to prepare zeolites [4,14,15] and hierarchical porous nano silica [16] for $CO_2$ adsorption. The COFA-derived inert supports for $K_2CO_3$-based, CaO-based, or amine-based sorbents for $CO_2$ capture are also reported [17–19].

In this paper, the literature on $CO_2$ sequestration using COFA has been comprehensively reviewed. The reviewed $CO_2$ sequestration technologies majorly include direct and indirect wet carbonation, synthesis of porous $CO_2$ adsorbents derived from COFA, and the development of COFA-derived inert supports for gas-solid adsorbents. The detailed technical route and important findings regarding the above $CO_2$ sequestration techniques are described. Moreover, the carbonation efficiency of COFA using different sequestration technologies and the practicality of these potential technical routes are comparatively discussed. The major aim of this review is to timely grasp the development status and technical challenges of $CO_2$ sequestration technologies using COFA and provide suggestions on the future development of these technologies.

## 2. $CO_2$ Mineralization

The specific flow chart of direct and indirect $CO_2$ mineralization using COFA is depicted in Figure 1. The $CO_2$ sequestration is mainly accomplished by mineralization in a slurry (direct carbonation) or aqueous solution (indirect carbonation). The relevant research on direct and indirect $CO_2$ mineralization using COFA is described in detail below.

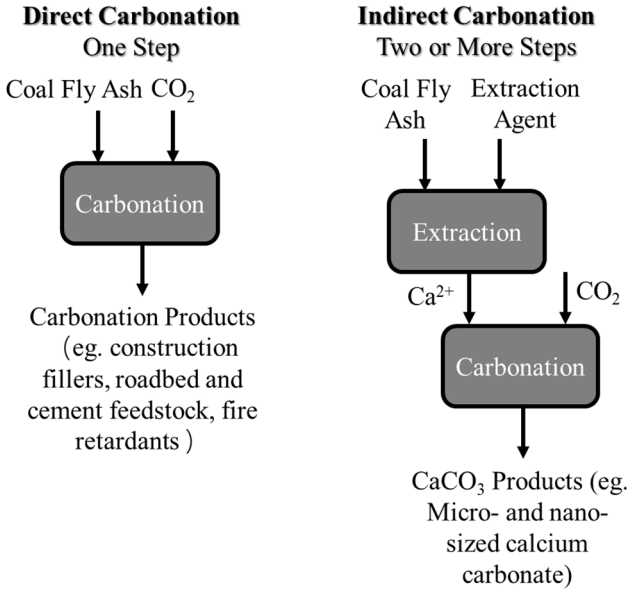


**Figure 1.** Flow chart of direct and indirect $CO_2$ mineralization using COFA [13]. Copyright 2012, with permission from Elsevier.

### *2.1. Direct Carbonation*

Direct $CO_2$ mineralization is achieved by the reaction of COFA and $CO_2$ either in a gaseous or aqueous phase environment. The direct $CO_2$ mineralization route is simple and potential, and it possesses the advantages of eliminating the extraction step of reactive components and the minimal consumption of chemical reagents. As listed in Table 1, research on the direct $CO_2$ mineralization of COFA is mainly centered on the investigation of $CO_2$ sequestration parameters such as COFA component, carbonation temperature, carbonation pressure, carbonation time, liquid-to-solid ratio, etc. [1,9]. Moreover, there are

also studies on adding calcium and magnesium ion extractants or using supercritical $CO_2$ to promote fly ash direct mineralization to fix $CO_2$.

As illustrated in Figure 2, the carbonation process of COFA mineralizing $CO_2$ mainly includes three stages [20]: (I) dissolution of $CO_2$ in fly ash slurry and ionization of $H_2CO_3$ produces $CO_3^{2-}$; (II) $Ca^{2+}$ and $Mg^{2+}$ leaching into solution; (III) generation of $CaCO_3/MgCO_3$ grains that are wrapped on the surface of fly ash particles or dispersed in slurry. In fact, the carbonation reaction gradually penetrates from the outside surface to the inner core of COFA particles. Gaseous $CO_2$ is diffused and dissolved in the liquid film surrounding the fly ash particles and reacts by leaching out $Ca^{2+}$ and $Mg^{2+}$. The generated carbonate products deposit on the surface of fly ash particles, leading to an uncarbonated inner core surrounded by a growing edge of carbonate products [21]. Therefore, the parameters of $Ca^{2+}/Mg^{2+}$ leaching and transportation, $CO_2$ diffusion, carbonate product coating, and pore blockage will affect the overall rate and degree of the carbonation reaction. Among them, $Ca^{2+}/Mg^{2+}$ leaching is the rate-limiting step of COFA mineralizing $CO_2$.

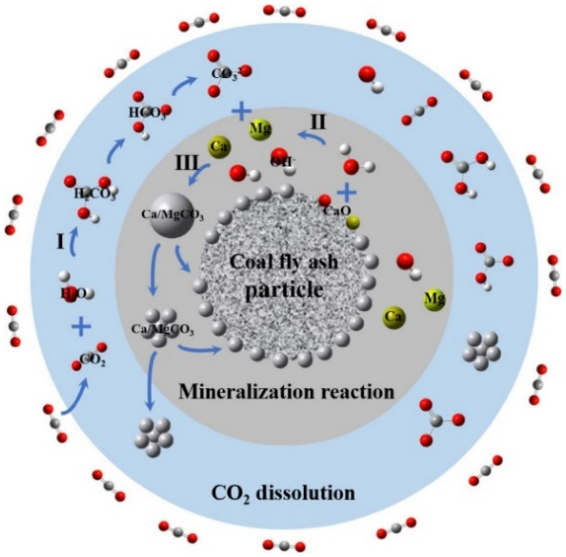


**Figure 2.** Carbonation reaction mechanism of COFA directly mineralizes $CO_2$ [20]. Copyright 2023, with permission from Elsevier.

The in-situ naturally weathered COFA in a wet-dumped ash dam can achieve $CO_2$ sequestration via carbonation to some extent; however, the carbonation reaction rate is too slow. Muriithi et al. [22] found that a period of 20 years was required to capture 6.8 wt% $CO_2$ by in-situ natural carbonation of wet disposed ash. In contrast, the fresh COFA fixed 6.5 wt% $CO_2$ via ex-situ accelerated carbonation (i.e., 4 Mpa, 90 °C, and liquid/solid ratio of 1 mL/g) in merely 2 h. Therefore, ex-situ accelerated carbonation of COFAes is a promising large-scale $CO_2$ sequestration technology.

There are great discrepancies in the components of COFA due to the different coal types and the ways of flue gas desulfurization. The content of alkaline earth metals within COFAes closely affects their $CO_2$ sequestration capacity ($C_n$), especially the Ca content. Ji et al. [23] dedicated themselves to studying the COFA properties' influence on the carbonation reactions, and five types of Chinese and Australian coal combustion fly ashes were used as the samples for the study. It was found that the rich reactive Ca/Mg-bearing crystalline phases in COFA, such as CaO, $Ca(OH)_2$, MgO, and $Ca_2Fe_2O_5$ and $Mg(OH)_2$, contributed to the increased $C_n$. Particularly, the Ca-bearing phases were superior to the Mg-bearing phases in improving the kinetics of carbonation reactions due to their higher reactivity with $CO_2$. The COFA containing 32.4 wt% of CaO and 29.3 wt% of MgO exhibited the highest $C_n$ of 132 g-$CO_2$/kg-fly ash via accelerated carbonation (carried out at 220 °C, initial $CO_2$ pressure of 2 MPa, 2 h and a liquid/solid ratio of 5 mL/g).

Moreover, Yuan et al. [24,25] selected four types of fly ashes derived from the subcritical, supercritical, and ultra-supercritical units, respectively, and the circulating fluidized bed, drum, and once-through boiler units. It was found that the raw fly ashes exhibited extremely low $C_n$ of 1.8 g $CO_2$/kg fly ash via dry mineralization. Mechanical ball milling modification could effectively enhance the $C_n$ of fly ashes due to producing more fresh surfaces and pores within fly ashes. The $CO_2$ sequestration capacities of wet and dry milling-modified ashes were, respectively, increased to 12.9 and 37.1 g $CO_2$/kg fly ash [24]. In addition, wet mineralization is markedly superior to dry mineralization in improving the $C_n$ of fly ashes. Even the raw fly ashes displayed outstanding $C_n$ under the wet mineralization route, which was significantly better than that of mechanically modified fly ashes under dry mineralization conditions. It was mainly ascribed to the presence of water effectively accelerating the leaching of $Ca^{2+}$/$Mg^{2+}$ from the solid COFA particles in wet mineralization conditions [26], consequently the superior $C_n$. Although the water availability promotes the leaching of $Ca^{2+}$/$Mg^{2+}$, excess water slowed the $CO_2$ diffusion rate due to the formed mass transfer barrier blocking the pores and cavities on the fly ash particles' surfaces, instead reducing the carbonation efficiency. Moreover, the high reaction temperature contributed to the accelerated carbonation reaction due to the improved mass transfer rate, thermal movement of molecules, and average reaction kinetics [27,28]. However, the low $CO_2$ solubility in water and the exothermic carbonation reaction were not conducive to $CO_2$ sequestration at high temperatures.

To further break through the bottleneck of slow carbonation rate in the $CO_2$ mineralization process of COFA, supercritical $CO_2$ was adopted to enhance carbonation [24,25]. The COFA exhibited a markedly higher $C_n$ under supercritical $CO_2$ (54.9 g $CO_2$/kg fly ash) compared to non-supercritical $CO_2$ (42.3 g $CO_2$/kg fly ash) due to the supercritical $CO_2$ possessing the advantages of strong diffusion character and desirable permeability. The $CO_2$ mineralization experiments of block CaO were designed by Yuan et al. [25] to measure the diffusion characteristics of supercritical and non-supercritical $CO_2$. As illustrated in Figure 3, the supercritical $CO_2$ (128.6 μm) exhibited a significantly deeper diffusion depth than the non-supercritical $CO_2$ (105.5 μm) within block CaO, intuitively demonstrating the strong diffusion characteristics.

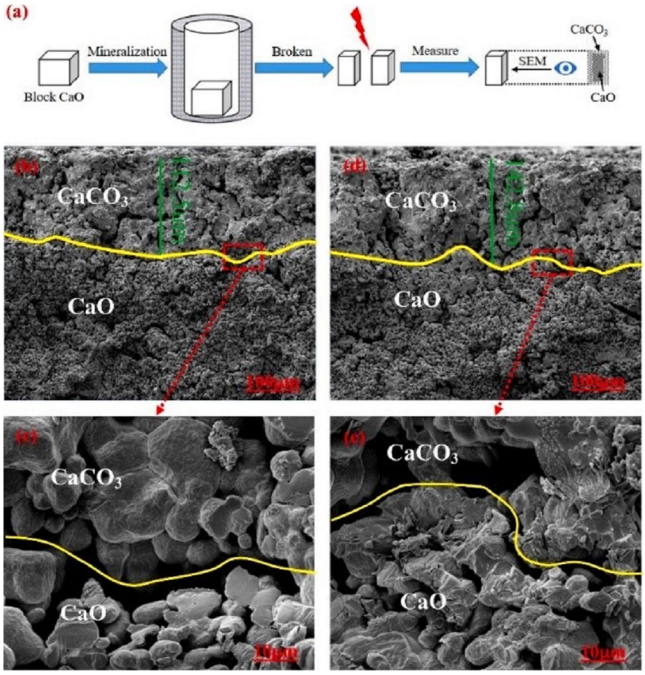


**Figure 3.** (**a**) Sketch map of measuring the $CO_2$ diffusion distance within block CaO, morphology images of (**b**,**c**) non-supercritical $CO_2$, (**d**,**e**) supercritical $CO_2$ [25]. Copyright 2022, with permission from Elsevier.

Siriwardena et al. [29] conducted experiments to measure the carbonation coefficient of cylindrical specimens (19 × 38 mm) of fly ashes. The fly ash specimens were placed in the carbonation chamber under certain conditions (reactor temperature of 40 ± 1 °C, relative humidity of 65 ± 5%, and $CO_2$ concentration of 5 ± 0.5%). The carbonated specimens were split lengthwise, and the newly cut section was sprayed with 1% phenolphthalein indicator. The depth of carbonation could be evaluated by measuring the depth to the color boundary line between the carbonated (pH < 9.2, colorless) and uncarbonated (pH > 9.2, purple) regions, as shown in Figure 4. The following diffusion equation can describe the relationship between carbonation depth and exposure period.

$$X = C\sqrt{t} + a \quad (1)$$

where X refers to the depth of carbonation (cm); C is the coefficient of carbonation ($cm\sqrt{days}$); $t$ represents the duration of accelerated carbonation (days); and $a$ is the empirical constant (cm). Although the COFA exhibited relatively low $C_n$ (~41.6 g $CO_2$/kg fly ash), the progression of carbonation in COFA was rapid, exhibiting a significantly high carbonation coefficient of $1.66cm\sqrt{days}$. It was mainly attributed to the less dense matrix in fly ash specimens, which allowed rapid diffusion of $CO_2$ because of the generation of fewer reaction products.

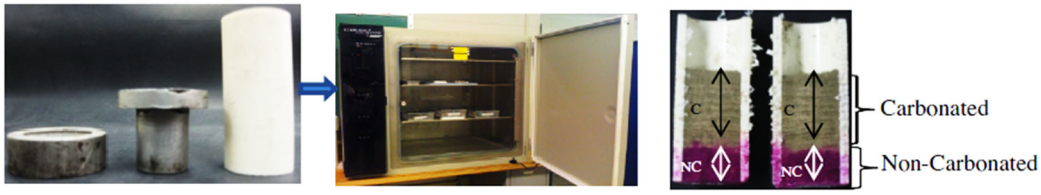


**Figure 4.** Procedure for the determination of carbonation depth [29]. Copyright 2015, with permission from Elsevier.

The other researchers also conducted many experimental studies to reveal the effect of $CO_2$ mineralization parameters on the $C_n$ of coal fly ashes. However, the reported values of $C_n$ varied in different studies due to the different selected fly ashes and $CO_2$ mineralization parameters (Table 1) [30–41]. As shown in Figure 5, Pan et al. [32] proposed an integrated route for $CO_2$ sequestration, fly ash stabilization, and by-product application using a high-gravity carbonation treatment method. The influence of different operating parameters on the carbonation conversion of COFA was investigated by response surface methodology. The maximal carbonation conversion of fly ash was 77.2% (i.e., $C_n$ of 249.4 g $CO_2$/kg fly ash) using a rotation rate of 743 rpm and a liquid/solid ratio of 18.9 mL/g at 57.3 °C. Moreover, the physicochemical properties (i.e., heavy metal leaching and volume expansion) of carbonated fly ash were upgraded, making them suitable for green materials in construction engineering.

The leaching of $Ca^{2+}$ and $Mg^{2+}$ into solution is an important parameter that affects carbonation efficiency. Therefore, the addition of $Ca^{2+}$ and $Mg^{2+}$ extractants is an effective approach to promote the leaching of $Ca^{2+}$ and $Mg^{2+}$ into the solution, resulting in improved $C_n$. Ji et al. [42] studied the effect of various 0.5 mol/L additives (i.e., $Na_2CO_3$, $Na_2CO_3$, and NaCl, $NaHCO_3$) on the $CO_2$ sequestration efficiency of coal fly ashes. The carbonation efficiency for different additives was ranked in the following order: 0.5 mol/L $Na_2CO_3$ > 0.5 mol/L $Na_2CO_3$ and 0.5 mol/L NaCl > 0.5 mol/L $NaHCO_3$. The $C_n$ was as high as 102 g $CO_2$/kg fly ash under the conditions of 0.5 mol/L $Na_2CO_3$ and liquid/solid ratio of 10 mL/g at 275 °C and 2 MPa for 2 h. It was mainly attributed to $Na_2CO_3$, which can provide abundant $CO_3^{2-}$ in the liquid phase, which results in superior $C_n$. The $C_n$ of COFA with the addition of 1 mol/L $NH_4Cl$ or sea salt was comparatively studied by Jo et al. [43]. It was suggested that the additives increase the solubility of Ca-bearing minerals, resulting in more $CO_2$ sequestration to some extent. Therefore, the $C_n$ in the presence of 1 mol/L

$NH_4Cl$ with a liquid/solid ratio of 3 mL/g at 25 °C for 18 h was approximately 23 g $CO_2$/kg fly ash, compared to 19 g $CO_2$/kg fly ash in its absence.

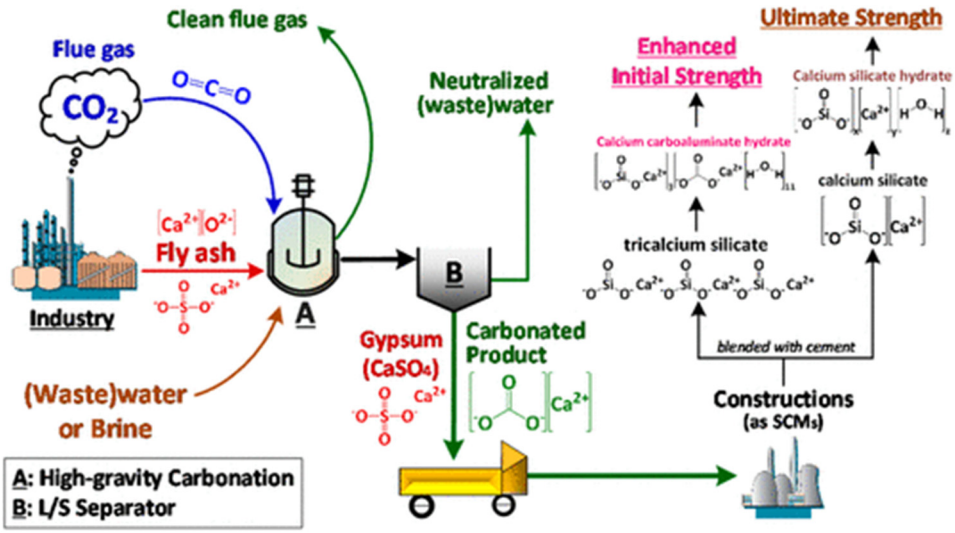


**Figure 5.** Schematic diagram of integrated $CO_2$ sequestration, circular fluidized bed fly ash stabilization, and by-product application via high-gravity carbonation process [32]. Copyright 2016, with permission from the American Chemical Society.

The amine-looping process using coal fly ash could achieve efficient $CO_2$ mineralization as well, which was confirmed in the study by Ji et al. [44,45]. They mainly investigated the $CO_2$ fixation performance of COFA in various typical amine solutions (i.e., monoethanolamine, diethanolamine, triethanolamine, 2-amino-2-methy-1-propanol, and piperazine). It revealed that amines contributed to enhancing the mass transfer of $CO_2$, promoting $Ca^{2+}$ leaching, and generating small $CaCO_3$ precipitation particles, especially the fly ash in 0.5 mol/L piperazine solution, which exhibited the desirable $C_n$ of 102.9 g $CO_2$/kg fly ash. The mechanism of amine-looping for high-efficiency $CO_2$ carbonation in the water system using COFA was illustrated in Figure 6. The $CO_2$ sequestration was a three-step process: mass transfer of the gaseous $CO_2$ phase to the aqueous $CO_2$ phase, leaching of $Ca^{2+}$, and precipitation of $CaCO_3$. Amines promoted the mass transfer of the gaseous $CO_2$ phase to the aqueous $CO_2$ phase by providing extra $CO_2$ reaction pathways. Meanwhile, the protonated amines formed from carbamate generation enhanced the leaching of $Ca^{2+}$, therefore being beneficial for the precipitation of $CaCO_3$. Piperazine (a typical diamine) could offer two amino groups used to adsorb $CO_2$, which can maintain a markedly higher $CO_2$ concentration in the solution compared to the other four monoamines, resulting in superior $CO_2$ sequestration performance.

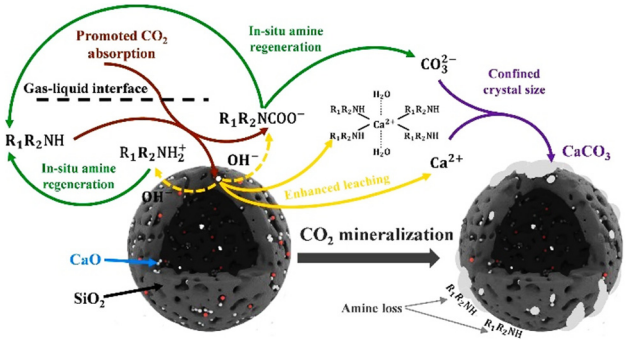


**Figure 6.** Mechanism of high-efficiency $CO_2$ mineralization using COFA based on amine-looping [44]. Copyright 2022, with permission from Elsevier.

To overcome the issue of the large energy consumption of absorbent regeneration for the amine-looping process, an integrated process combining $CO_2$ absorption with mineralization was proposed [45]. A chemical method was used to regenerate the amine absorbent in the integrated process combining $CO_2$ absorption with mineralization rather than the traditional thermal method. As shown in Figure 7, the $CO_2$-rich solution was sent to the carbonation sink, where carbonation reactions occurred between the CaO-rich wastes and the $CO_2$-rich solution. Afterward, the $CO_2$ was sequestered as a solid $CaCO_3$ phase, and the amine solvent was regenerated and returned to the absorption reactor for continuous $CO_2$ absorption. The practical application of using COFA as a feedstock for the regeneration of absorbent in an integrated $CO_2$ absorption-mineralization process was feasible. Results indicated that piperazine showed a larger cyclic loading of 0.42 mol/mol in the integrated process, which was approximately more than 1.1 times that of the traditional regeneration process by a thermal method.

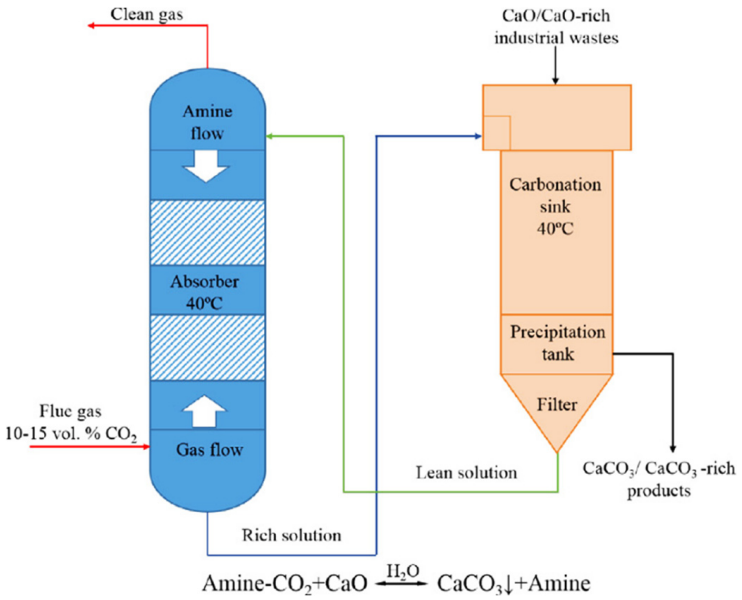


**Figure 7.** Process flow sheet of the integrated process combining $CO_2$ absorption with mineralization [45]. Copyright 2018, with permission from Elsevier.

**Table 1.** Summary of direct $CO_2$ mineralization using COFA.

| Reference | Carbonation Condition | CaO and MgO Content in Fly Ash | $C_n$ (g-$CO_2$/kg-Fly Ash) |
|---|---|---|---|
| Shao et al. [20] | liquid/solid ratio of 6 mL/g, 30 °C, initial $CO_2$ pressure of 2 MPa, 15 min | 8.8 wt% Ca, 0.36 wt% Mg | 54.9 |
| Muriithi et al. [22] | brine, liquid/solid ratio of 1 mL/g, 90 °C, initial $CO_2$ pressure of 4 MPa, 30 vol % $CO_2$, 2 h | 9.2 wt% Ca, 2.44 wt% Mg | 65 |
| | in-situ natural carbonation, 20 years | | 68 |
| Yuan et al. [24] | 100 rpm, liquid/solid ratio of 100 mL/g, 80 °C, initial $CO_2$ pressure of 1 MPa, 5 h | 25.83 wt% CaO, 2.17 wt% MgO | 42.3 |
| | 100 rpm, liquid/solid ratio of 30 mL/g, 40 °C, initial $CO_2$ pressure of 8 MPa, 5 h | | 54.9 |
| | 100 rpm, dry mineralization, 40 °C, initial $CO_2$ pressure of 8 MPa, 5 h | | 1.8 (raw ashes)<br>12.9 (dry milled ashes)<br>37.1 (wet milled ashes) |

**Table 1.** *Cont.*

| Reference | Carbonation Condition | CaO and MgO Content in Fly Ash | $C_n$ (g-$CO_2$/kg-Fly Ash) |
|---|---|---|---|
| Yuan et al. [25] | 100 rpm, dry mineralization, 40 °C, initial $CO_2$ pressure of 8 MPa, 1 h | 10.37 wt% CaO, 2.17 wt% MgO | 1.8 |
| | 100 rpm, liquid/solid ratio of 10 mL/g, 40 °C, initial $CO_2$ pressure of 3, 5 and 8 MPa, 1 h | 10.37 wt% CaO, 2.17 wt% MgO | 55 (3 MPa), 58.2 (5 MPa), 89.3 (8 MPa) |
| | 100 rpm, liquid/solid ratio of 10 mL/g, 40 °C, initial $CO_2$ pressure of 3, 5 and 8 MPa, 1 h | 6.67 wt% CaO, 0.84 wt% MgO | 19.7 (3 MPa), 23.8 (5 MPa), 38.3 (8 MPa) |
| | 100 rpm, liquid/solid ratio of 10 mL/g, 40 °C, initial $CO_2$ pressure of 3, 5 and 8 MPa, 1 h | 6.55 wt% CaO, 1.14 wt% MgO | 17.5 (3 MPa), 19.4 (5 MPa), 35.5 (8 MPa) |
| | 100 rpm, liquid/solid ratio of 10 mL/g, 40 °C, initial $CO_2$ pressure of 3, 5 and 8 MPa, 1 h | 4.68 wt% CaO, 0.24 wt% MgO | 10.7 (3 MPa), 11.7 (5 MPa), 13.9 (8 MPa) |
| Ji et al. [23] | liquid/solid ratio of 5 mL/g, 220 °C, initial CO2 pressure of 2 MPa, 2 h | 16.4 wt% CaO, 1.2 wt% MgO | 58 |
| | liquid/solid ratio of 5 mL/g, 220 °C, initial $CO_2$ pressure of 2 MPa, 2 h | 9.4 wt% CaO, 27.9 wt% MgO | 125 |
| | liquid/solid ratio of 5 mL/g, 140 °C, initial $CO_2$ pressure of 2 MPa, 2 h | 3.6 wt% CaO, 7.1 wt% MgO | 13 |
| | liquid/solid ratio of 5 mL/g, 140 °C, initial $CO_2$ pressure of 2 MPa, 2 h | 13.4 wt% CaO, 0.5 wt% MgO | 26.5 |
| | liquid/solid ratio of 5 mL/g, 220 °C, initial $CO_2$ pressure of 2 MPa, 2 h | 32.4 wt% CaO, 29.3 wt% MgO | 132 |
| Siriwardena et al. [29] | liquid/solid ratio of 0.3 mL/g, 40 °C, 10 vol % $CO_2$, humidity of 65%, 28 days | 22.75 wt% CaO, 4.48 wt% MgO | 41.6 |
| Back et al. [30] | 600 rpm, liquid/solid ratio of 20 mL/g, 75 °C, initial $CO_2$ pressure of 0.01 MPa, 4.5 h | 37.3 wt% CaO,15.4 wt% MgO | 230 |
| La Plante et al. [31] | liquid/solid ratio of 100 mL/g, atmospheric pressure, 60 °C, 100 vol % $CO_2$, 72 h | 28.5 wt% CaO, 6.6 wt% MgO | 95.0 |
| Pan et al. [32] | 743 rpm, liquid/solid ratio of 18.9 mL/g, 57.3 °C, 15 vol % $CO_2$ | 62.8 wt% CaO, 0.83 wt% MgO | 249.4 |
| Revathy [33] | liquid/solid ratio of 13.35 mL/g, 61.6 °C, 4.87 MPa, 100 vol % $CO_2$, 50 min | 6.74 wt% CaO | 50.72 |
| Ukwattage et al. [34] | liquid/solid ratio of 5 mL/g, 40 °C, initial $CO_2$ pressure of 6 MPa, 10 h | 39.8 wt% CaO, 7.3 wt% MgO | 7.66 |
| Miao et al. [35] | liquid/solid ratio of 10 mL/g, 5 kWh/m3 energy input in slurry, 60 °C, 15 vol % $CO_2$, 2 h | 33.1 wt% CaO, 0.95 wt% MgO | 128 |
| Montes-Hernandez et al. [36] | liquid/solid ratio of 10 mL/g, 30 °C, initial $CO_2$ pressure of 1 MPa, 18 h | 5.0 wt% CaO | 26.2 |
| Bauer et al. [37] | 1500 rpm, liquid/solid ratio of 0.12 mL/g, 25–80 °C, initial $CO_2$ pressure of 0.015 MPa, 2 h | 28.4 wt% Ca, 0.92 wt% Mg | 211 |
| Ukwattage et al. [38] | 60 rpm, liquid/solid ratio of 3 mL/g, 60 °C, initial $CO_2$ pressure of 3 MPa, 10 h | 24.8 wt% CaO, 13 wt% MgO | 27.1 |
| Dananjayan et al. [39] | 900 rpm, liquid/solid ratio of 15 mL/g, 30 °C, initial $CO_2$ pressure of 0.4 MPa, 2 h | 6.74 wt% CaO, 2.22 wt% MgO | 50.3 |
| Patel et al. [40] | liquid/solid ratio of 0.24 mL/g, 50 °C, 30 vol % $CO_2$ | 37.25 wt% CaO, 0.45 wt% MgO | 40 |

**Table 1.** *Cont.*

| Reference | Carbonation Condition | CaO and MgO Content in Fly Ash | $C_n$ (g-$CO_2$/kg-Fly Ash) |
|---|---|---|---|
| Ho et al. [41] | liquid/solid ratio of 100 mL/g, atmospheric pressure room temperature, 30 vol % $CO_2$, 30 min | 3.44 wt% Ca, 0.82 wt% Mg | 16 |
| Nyambura et al. [46] | brine, 600 rpm, liquid/solid ratio of 2 mL/g, 30 °C, initial $CO_2$ pressure of 4 MPa, 2 h | 9.2 wt% Ca, 2.44 wt% Mg | 71.8 |
| Jo et al. [43] | deionized water, liquid/solid ratio of 3 mL/g, 25 °C, 15 vol % $CO_2$, 18 h | 7.2 wt% CaO, 1.5 wt% MgO | 19 |
| | 1 M $NH_4$ Cl, liquid/solid ratio of 3 mL/g, 25 °C, 15 vol % $CO_2$, 18 h | | 23 |
| | sea water, liquid/solid ratio of 3 mL/g, 25 °C, 15 vol % $CO_2$, 18 h | | 20 |
| Ji et al. [42] | 0.5 M $Na_2CO_3$, liquid/solid ratio of 10 mL/g, 275 °C, initial $CO_2$ pressure of 2 MPa, 2 h | 16.4 wt% CaO, 1.2 wt% MgO | 102 |
| Ji et al. [44] | 0.5 mol/L piperazine solution, liquid/solid ratio of 10 mL/g, atmospheric pressure, 55 °C, 40 vol % $CO_2$, 1.5 h | 24.3 wt% CaO, 0.9 wt% MgO | 102.9 |

### *2.2. Indirect Carbonation*

Indirect mineral carbonation of coal fly ashes mainly involves the extraction of $Ca^{2+}$ by acids or other solvents into an aqueous solution, followed by the carbonation reaction between the extracted $Ca^{2+}$ and injected $CO_2$. Indirect mineral carbonation allows for the production of pure carbonates due to the impurities (i.e., Si and Fe) that can be filtered out prior to carbonate precipitation [47].

He et al. [48,49] explored the effect of various extraction agents (i.e., $NH_4Cl$, $NH_4NO_3$, and $CH_3COONH_4$) on $Ca^{2+}$ extraction efficiency from COFA particles. The above three ammonia salts were all effective $Ca^{2+}$ extraction agents, achieving a calcium leaching efficiency of about 35–40% within 1 h. $CH_4COONH_4$ was superior to the other two ammonia salts in promoting $Ca^{2+}$ extraction of COFA. A carbonation efficiency of 41–47% was achieved when carbonating the leachate with $CO_2$. Furthermore, a higher carbonation efficiency of ~90–93% can be obtained when $NH_4HCO_3$ is used instead of $CO_2$ as the source of $CO_3^{2-}$. By this method, 1 ton of fly ash could sequester 0.075 t of $CO_2$, simultaneously producing 0.17 t of precipitated $CaCO_3$. Jo et al. [50] investigated the effect of solid dosage, CaO content, $CO_2$ flow rate, and solvent type on the extraction efficiency of $Ca^{2+}$ from coal fly ashes. In fact, the extraction efficiency of $Ca^{2+}$ was closely associated with the ultimate carbonation efficiency of fly ash. The results indicated that the $C_n$ of fly ash was about 8 g-$CO_2$/kg-fly ash using deionized water as the solvent at ambient temperature and pressure conditions with a solid dosage of 100 g/L and a $CO_2$ flow rate of 2 mL/min.

Moreover, acetic acid was also used as the leachate to extract $Ca^{2+}$ and $Mg^{2+}$ from brown COFA to achieve indirect $CO_2$ mineralization sequestration [51]. Most of the Ca and Mg within COFA could be dissolved into the solution at the initial stage of leaching, and the carbonation of the leached solution was conducted using a continuously stirred high-pressure autoclave. The $CO_2$ was sequestered mainly in carbonate precipitates (i.e., $CaCO_3$ and $MgCO_3$) and water-soluble bicarbonate (i.e., $Mg(HCO_3)_2$). The carbonation of brown COFA-derived leachate exhibited a markedly lower global activation energy of 12.7 kJ/mol compared to that of natural minerals, contributing to maintaining a fast reaction rate. As shown in Figure 8, the maximum $C_n$ of the fly ash was obtained at 60 °C for either $CO_2$ being sequestrated in the form of the solid or liquid phase. Therefore, the maximum $C_n$ could reach 264 g $CO_2$/kg fly ash when considering both the contributions of

carbonate precipitates and water-soluble bicarbonate. In addition, multiple-cycle leaching-carbonation and $Mg^{2+}$ leaching kinetic modeling were studied during indirect carbonation of Victorian brown COFA for $CO_2$ fixation [47]. It revealed that the extraction efficiency of $Ca^{2+}$ and $Mg^{2+}$ markedly decreased with the increased cycling number of ammonium chloride. The carbonation efficiency gradually dropped with the increase in ammonium chloride cycles as well.

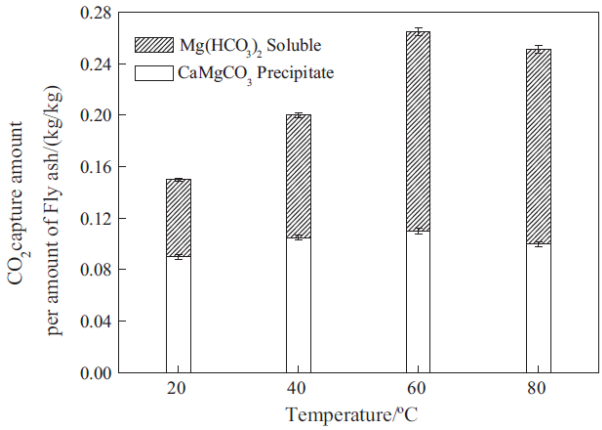


**Figure 8.** Impact of carbonation temperature on $CO_2$ uptake at 10 bar [51]. Copyright 2012, with permission from Elsevier.

An integrated circular system combining indirect carbonation of COFA with solution regeneration by bipolar membrane electrodialysis (BPED) was put forward by Ho et al. [52]. As shown in Figure 9, the system consisted of three main blocks, i.e., $Ca^{2+}$ leaching from fly ash, $CaCO_3$ precipitation, and acid and alkaline solution regeneration. The $CO_2$ sequestration mechanism of COFA is described in Equation (2).

$$\text{Leachate solution}\left(Ca^{2+} + 2NO_3^-\right) + CO_2 \text{ capture solution}\left(2Na^+ + CO_3^{2-}\right) \rightarrow CaCO_{3(s)} + 2NaNO_{3(aq)} \quad (2)$$

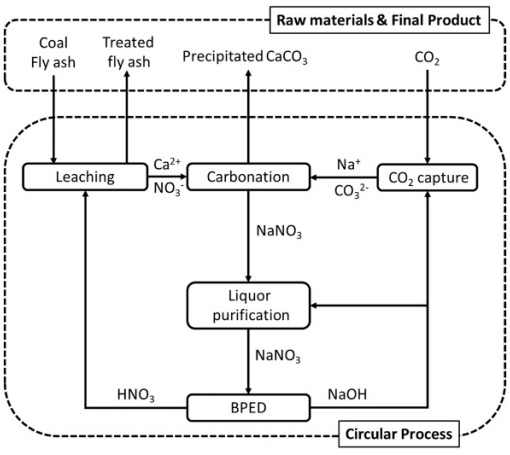


**Figure 9.** The integrated system of circular indirect carbonation of coal fly ashes [52]. Copyright 2022, with permission from Elsevier.

BPED could regenerate the $HNO_3$ and NaOH solutions (Equation (3)). The bipolar membranes could decompose the water into $H^+$ and $OH^-$, and simultaneously dissociate the salt into $Na^+$ and $NO_3^-$ through electrodialysis, consequently regenerating the $HNO_3$ and NaOH solutions.

$$NaNO_{3(aq)} + H_2O \rightarrow NaOH(\text{for } CO_2 \text{ capture}) + HNO_3(\text{for leaching}) \quad (3)$$

The experiment results demonstrated that the $C_n$ was ~11 g $CO_2$/g fly ash, corresponding to a $CO_2$ conversion of 92.9%. During the leaching stage, the adoption of a relatively lower nitric acid/calcium ratio was beneficial to the generation of a higher-purity $CaCO_3$ precipitate.

A novel electrolytic carbonation system for the collaborative treatment of COFA, brine wastewater, and $CO_2$ was proposed by Lu et al. [53]. As shown in Figure 10, the acidity produced by the electrolysis of brine electrolyte at the anode directly leached $Ca^{2+}$ or $Mg^{2+}$ from COFA. The $Ca^{2+}$ or $Mg^{2+}$ balanced the $OH^-$ generated at the cathode to form $Ca(OH)_2$ or $Mg(OH)_2$, which then sequestered $CO_2$ and simultaneously produced high-purity carbonate precipitates. The electrolysis contributed to the enhanced dissolution of fly ash, and then it increased the $C_n$ from 9.75 to 18.42 g $CO_2$/kg fly ash in the NaCl electrolyte.

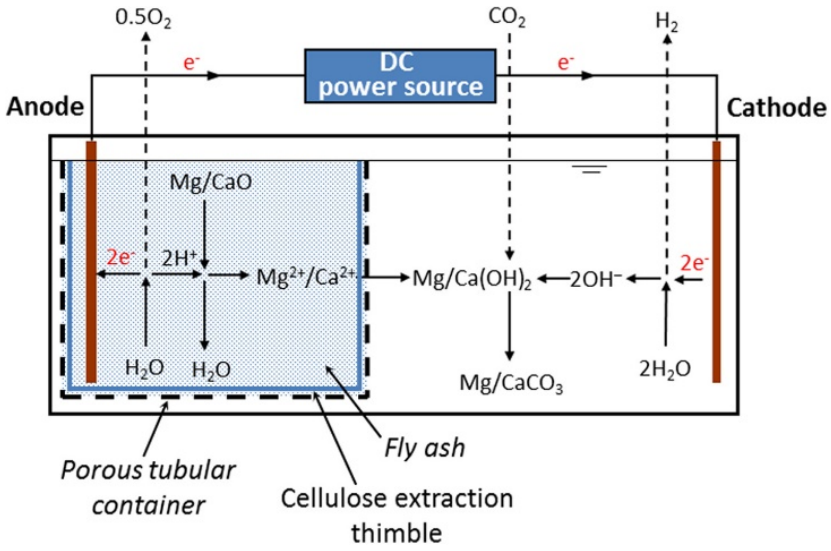


**Figure 10.** Schematic diagram of the electrolytic carbonation of COFA for in situ $CO_2$ sequestrate and mineral recovery [53]. Copyright 2016, with permission from Elsevier.

In addition, protonated amine [54] and glycine [55,56] were used as reagents during the COFA-based leaching-mineralization course, which avoided the large consumption of exogenous acid-base reagents. The protonated amine could promote $Ca^{2+}$ leaching from COFA, and simultaneously be converted into free amine [54]. Then, the free amine adsorbed the protons released by the precipitation reaction of $CaCO_3$ and could achieve in-situ regeneration of protonated amine. The authors systematically investigated the $CO_2$ mineralization performance of 13 typical amine-mediated COFA and the polymorph selection of $CaCO_3$. Triethanolamine (TEA) exhibited the largest $CaCO_3$ yield of 56.8%, and the corresponding Ca utilization efficiency was 16.8%. Moreover, the amines had a pronounced control effect on the $CaCO_3$ product's size, polymorph, and morphology. As shown in Figure 11, the primary amino group was superior to the secondary and tertiary ones in promoting the formation of vaterite. The introduction of a side chain was prone to make the vaterite transform to calcite, and the grain size of the vaterite was inversely proportional to the length of the side chain.

To achieve $CO_2$ sequestration and $CaCO_3$ production, Zheng et al. [55,56] designed a glycine-mediated leaching-mineralization method for COFA. The process can simultaneously achieve the desirable $CO_2$ sequestration efficiency of COFA and produce high-purity $CaCO_3$ products in an in-situ recyclable glycine solution. After leaching for 1 h, a mineralization efficiency of 74.4% and a maximum $CaCO_3$ yield of 98.8 g/kg fly ash were achieved in a 2 M glycine solution with a fly ash dosage of 200 g/L. The reaction mechanism of the glycine-mediated leaching-mineralization approach through glycine and COFA (COFA) was illustrated in Figure 12. During the leaching stage, Gly0 could act as the proton donor and chelating agent that markedly promoted $Ca^{2+}$ leaching, simultaneously producing $Gly^-$. As an excellent $CO_2$ absorbent, $Gly^-$ accelerates the mass transfer of gaseous $CO_2$ to

the liquid phase by offering extra $CO_2$ reaction pathways. The carboxyl of $Gly^-$ could also bind to the protons derived from carbonation reactions in the mineralization step, acting as a proton receptor. Moreover, the Gly species acted as a desirable crystal regulator in carbonate precipitation, which contributed to extending the continuous conversion and growth of $CaCO_3$ crystals.

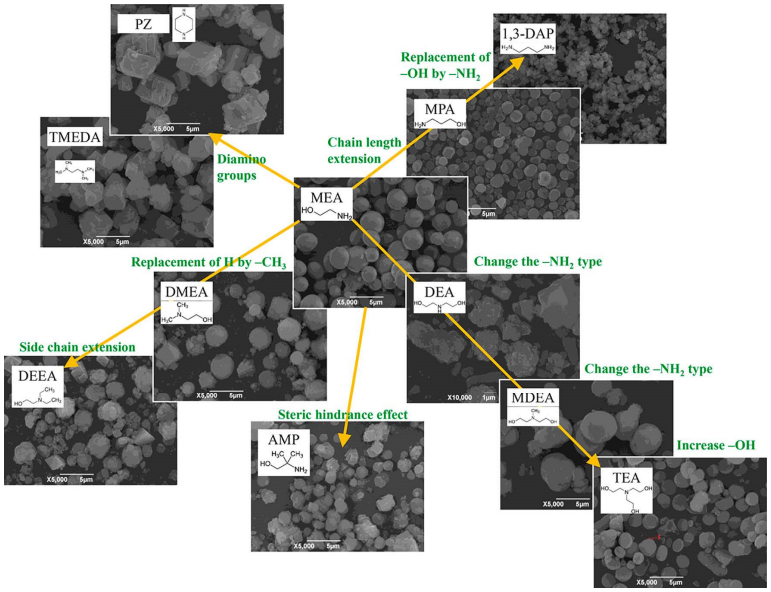


**Figure 11.** Surface morphology images of $CaCO_3$ induced by 11 types of selected amines [54]. Copyright 2022, with permission from Elsevier.

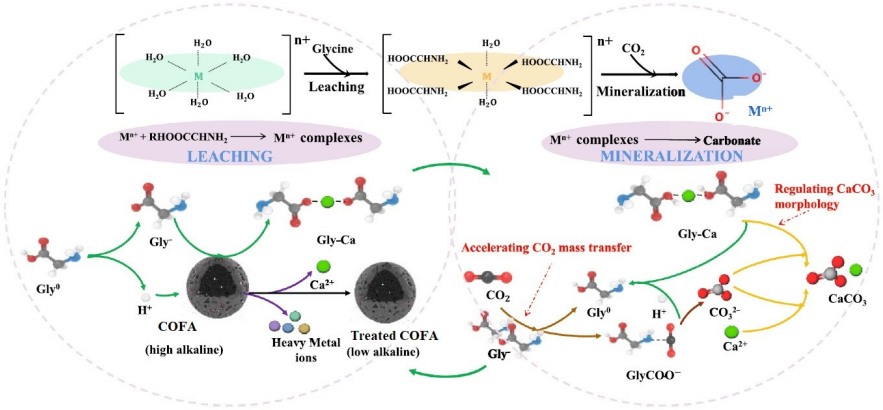


**Figure 12.** Mechanism of cyclic glycine-mediated leaching-mineralization approach using glycine and COFA [56]. Copyright 2022, with permission from Elsevier.

An integrated system coupling mineral carbonation with direct air capture under atmospheric conditions was put forward by Ragipani et al. [57], as depicted in Figure 13. The evenly mixed slurries of COFA and concentrated alkali carbonate were used as recyclable solvents. Sodium hydroxide solvent was used to sequestrate $CO_2$ (Equation (4)) during the DAC process. The Equations (5) and (6) described the reaction generating NaOH solution via the carbonation between the COFA and $Na_2CO_3$. conditions. It was found that the coupled system achieved a high $CaCO_3$ conversion of ~80% in a 1.9 M $Na_2CO_3$ solution for 1 h. Moreover, the cost of sequestering 1 ton of $CO_2$ was about \$116−133, while the process based on life cycle assessment emitted 0.03−0.25 t-$CO_2$e/t-$CO_2$-sequestered.

$$2NaOH_{(aq)} + CO_{2(g)} \rightarrow Na_2CO_{3(aq)} + H_2O \quad (4)$$

$$2CaO.SiO_{2(s)} + 2Na_2CO_{3(aq)} + 2H_2O \rightarrow 2CaCO_{3(s)} + SiO_{2(s)} + 4NaOH_{(aq)} \quad (5)$$

$$CaO.Al_2O_3.2SiO_{2(s)} + Na_2CO_{3(aq)} + 4H_2O \rightarrow CaCO_{3(s)} + 2Al\left(OH\right)_3 + 2SiO_{2(s)} + 2NaOH_{(aq)} \quad (6)$$

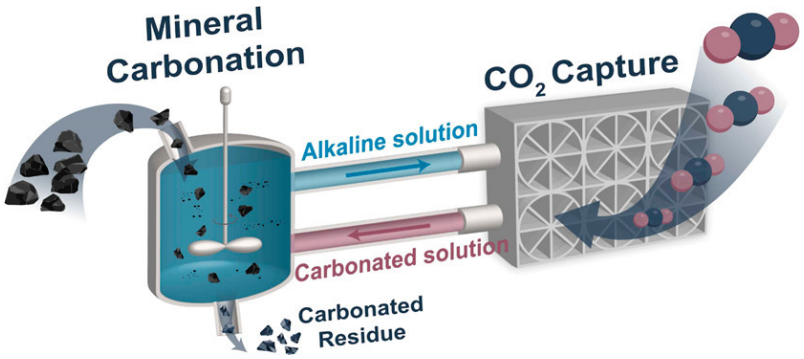


**Figure 13.** Schematic diagram of an integrated system coupling mineral carbonation with direct air capture under atmospheric conditions [57]. Copyright 2022, with permission from the American Chemical Society.

## 3. $CO_2$ Mineralization in Conjunction with Fly Ash-Derived by-Products Utilization

As mentioned above, the carbonation of COFAes can effectively achieve the fixation of $CO_2$. In addition, the further utilization of fly ash-derived by-products has also received extensive attention from researchers. Ren et al. [58] investigated the feasibility of combining the preparation of composite gravel with $CO_2$ absorption using COFA. The composite gravel pellets were prepared from mixtures of COFA, gypsum, Portland Cement and water, and the pellets were subjected to carbonation curing using flue gas. Figure 14a illustrates the prepared composite gravel pellets. The composite gravel pellets contained a 20 wt% cement content and 1:11(A11) ratio of gypsum to COFA, exhibiting the highest compressive strength of 11.11 MPa at the age of 28 days, as shown in Figure 14b. It was positively correlated with its $CO_2$ adsorption capacity, and the $CO_2$ adsorption for composite gravel pellets reached 4.789% with a 1:11 ratio of gypsum to COFA (Figure 14c).

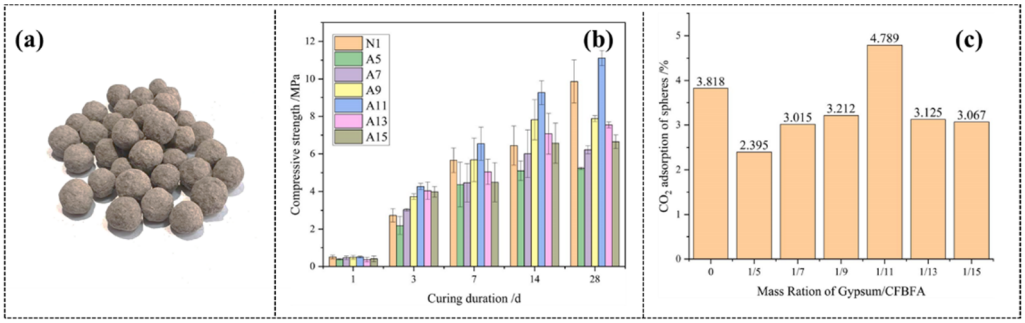


**Figure 14.** (**a**) Photo of composite gravels, (**b**) compressive strength of composite gravel with different curing durations, (**c**) $CO_2$ absorption capacity of composite gravel with different gypsum/COFA ratios [58]. Copyright 2023, with permission from Elsevier.

Moreover, a new approach of employing the carbonated slurry of coal fly ashes during the $CO_2$ sequestration process to inhibit spontaneous combustion of coal (SCC) in the coal mining process was put forward [20]. The COFA reached a $C_n$ of 54.9 g $CO_2$/kg fly ash with a liquid/solid ratio of 6 at 2 MPa. The carbonated fly ash slurry demonstrated a superior capability to inhibit SCC compared to the uncarbonated slurry. The temperature increase at the crossing point reached 13.8 °C in comparison to the origin coal when the carbonated fly ash slurry-to-coal ratio was set at 3:1. It greatly diminished the risk of

SCC, indicating carbonated fly ash slurry possessing an apparent suppression function on SCC. The carbonated coal fly ashes were used as the mineral admixture for concrete or cement mortar [59,60]. Chen et al. [60] studied the property of cement mortar containing carbonated coal fly ashes and the combined impact of carbonation curing. It showed that carbonation treatment decreased the proportion of free CaO and the hydration heat of coal fly ashes. Therefore, the expansion of mortar specimens incorporating carbonated fly ash was greatly mitigated in comparison to that of specimens using fresh fly ash [59]. In addition, Freire et al. [61] produced geopolymers with COFA and rice husk ash, which were adopted as the $CO_2$ capture materials, and various geopolymer formulations were tried. The calcined rice husk ash activated via NaOH was the best precursor to prepare geopolymer that exhibited superior $CO_2$ capture performance.

The dual needs of $CO_2$ emission reduction and COFA treatment require the design of an innovative pathway to simultaneously achieve $CO_2$ sequestration and further conversion into useful carbonates. Yin et al. [62] conducted a range of experiments using fly ash and a mixture of fly ash and bottom ash to study $CO_2$ mineralization function with regenerable solvents (i.e., 2.5 M sodium glycinate and 30 wt% MEA). A mixture of fly ash and bottom ash was superior to sole fly ash, which obtained the highest $CO_2$ mineralization degree of non-calcium carbonate content. Moreover, nanoscale calcium carbonate could be successfully produced from dissolved calcium through $CO_2$-loaded sodium glycinate and CTAB surfactant. The detailed reaction mechanism for the integrated approach of $CO_2$ mineralization and nanoscale calcium carbonate production using COFA was demonstrated in Figure 15. Therefore, the route of directly sequestering $CO_2$ in COFA and simultaneously producing nanoscale $CaCO_3$ with regenerable $CO_2$ capture solvents was feasible.

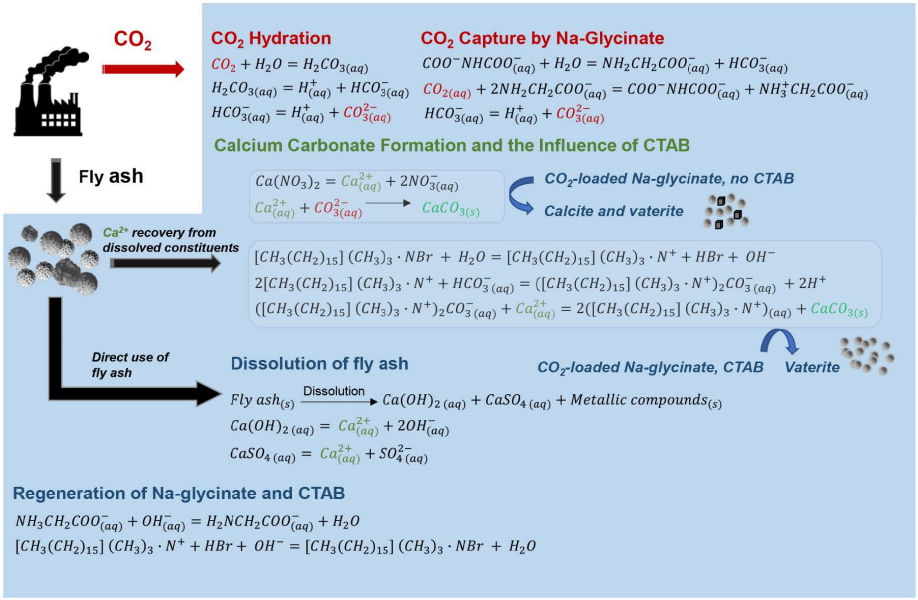


**Figure 15.** Schematic diagram of an integrated approach combining $CO_2$ capture with mineralization adopting sodium glycinate as a regenerable solvent and CTAB surfactant to control the size of $CaCO_3$ particles [62]. Copyright 2022, with permission from Elsevier.

In addition, Monasterio-Guillot et al. [63] were the first to explore the combined effects of $CO_2$ sequestration, zeolite production, and simultaneous heavy metal element trapping at the carbonation stage of COFA. The carbonation efficiency was as high as 79% (a net $C_n$ of 45 g $CO_2$/kg fly ash) c under mild hydrothermal conditions for Class F fly ash (3.72 wt% CaO, 1.74 wt% MgO). Simultaneously, the amorphous precursors of zeolite and different crystalline zeolites with a yield as high as 60 wt% were produced. The potentially toxic elements within COFA were effectively solidified in the newly generated calcite and zeolite products, avoiding the leaching of toxic elements.

As illustrated in Figure 16, a green and facile pathway to synthesize mesoporous γ-$Al_2O_3$ from COFA while simultaneously achieving on-site $CO_2$ utilization was investigated by Yan et al. [64]. The lime-sinter route was used to extract aluminum from COFA. The COFA mixed with $CaCO_3$ was calcined at 1390 °C and then the calcined products were dissolved in $Na_2CO_3$ solution at 70 °C, achieving a high aluminum extraction efficiency of 87.42%. Then, the flue gas containing 15 vol% $CO_2$ and 85 vol% $N_2$ after being purified was injected into the extracted liquid to achieve $CO_2$-assisted precipitation of $Al(OH)_3$ precursors (Equation (7)). Ultimately, the mesoporous γ-$Al_2O_3$ (high surface area of 230.3 $m^2.g^{-1}$) was produced by calcining the $Al(OH)_3$ at 400 °C or 550 °C (Equation (8)). This proposed pathway appeared to be desirable for scaled-up production of mesoporous γ-$Al_2O_3$ by integrating the on-site recycling of COFA and $CO_2$ utilization.

$$2NaAlO_{2(aq)} + CO_{2(g)} + 3H_2O \rightarrow Na_2CO_{3(aq)} + 2Al\left(OH\right)_{3(s)} \quad (7)$$

$$2Al\left(OH\right)_{3(s)} \rightarrow Al_2O_{3(s)} + 3H_2O \quad (8)$$

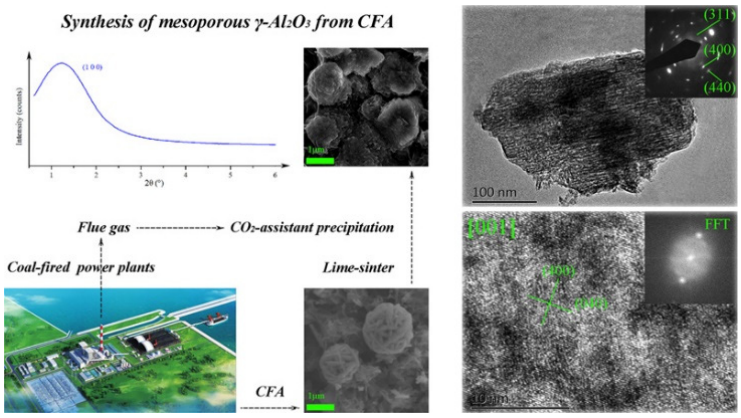


**Figure 16.** Mesoporous γ-$Al_2O_3$ synthesized from COFA combined with simultaneous on-site $CO_2$ utilization [64]. Copyright 2018, with permission from Elsevier.

## 4. $CO_2$ Sequestration of COFA by Dry Carbonation Process

In gas-solid carbonation, $CO_2$ reacts with free CaO within COFA to generate $CaCO_3$. Patel et al. [40] studied the $CO_2$ sequestration performance of COFA with reaction temperatures ranging from 500°C to 750 °C. Figure 17 demonstrated that the $CO_2$ sequestration level apparently increased with the temperature being leveled up to 700 °C in the initial stage. However, the $CO_2$ sequestration efficiency gradually dropped to below ~50% after the reaction time exceeding 10 min. Moreover, an apparent reduction in $CO_2$ sequestration efficiency was observed in the rapid reaction regime when the temperature reached 750 °C due to the simultaneous partial decomposition of $CaCO_3$.

Revathy et al. [33] designed the carbonation experiments of (Indian COFA (class F type-CaO < 10 wt%) via the gas-solid route using response surface methodology, and temperature and pressure were the main factors studied. The interaction between the factors (i.e., temperature and pressure) and their impacts on response (the reduction of $CO_2$ concentration) was analyzed. The temperature affected the carbonation efficiency of COFA because of the remarkable influence of temperature change on $CO_2$ concentration. At a certain temperature, the pressure played a profound role in the gas-solid carbonation of COFA. It was noted that the influence of temperature seemed to be more remarkable compared to that of pressure on the carbonation of fly ash when both temperature and pressure were changed. The global optimum solution was identified as a temperature of 44.86 °C and pressure of 24 bar, obtaining a reduction in $CO_2$ concentration of 18.2%. The COFA exhibited a maximum $C_n$ of 20.0 g $CO_2$/kg fly ash under gas-solid carbonation.

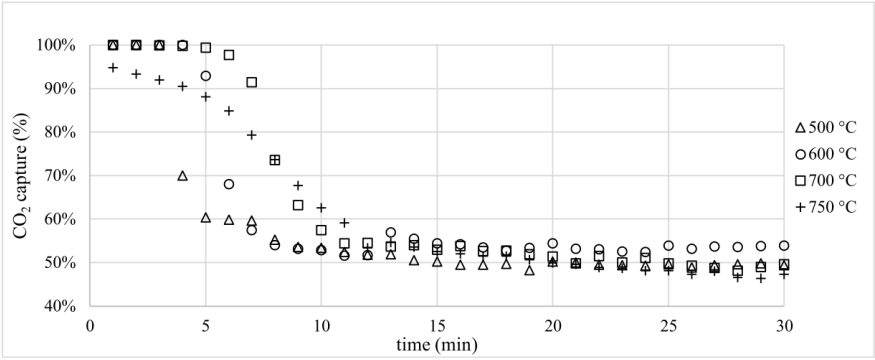


**Figure 17.** $CO_2$ sequestration capacities of dry COFA [40]. Copyright 2017, with permission from Elsevier.

Liu et al. [65] studied the influence of temperature, $CO_2$ concentration, steam concentration, and reaction duration on the $CO_2$ fixation performance of COFA via a direct gas-solid carbonation approach. It was found that the increased temperature and the concentration of $CO_2$ and $H_2O$(g) contributed to the improved $CO_2$ fixation efficiency. The effects of temperature and $H_2O$(g) were more apparent than that of $CO_2$ content. The COFA achieved a maximum $C_n$ of 60 g $CO_2$/kg fly ash corresponding to a fixation efficiency of 28.74% at 600 °C with 20% $H_2O$(g) addition. Moreover, Ćwik et al. [66] carried out a mineral carbonation experiment of high-calcium COFA using a continuous flow reactor with different temperatures and $CO_2$ pressures. The dry and moist conditions were comparatively investigated. Results exhibited that COFA achieved a maximal $C_n$ of 117.7 g $CO_2$/kg fly ash (corresponding to a carbonation efficiency of 48.14%) under gas-solid conditions. Moderate amounts of $H_2O$(g) contained in the $CO_2$ gas flow were beneficial to the improved carbonation efficiency. The promotion effect of steam resulted from the formation of $Ca(OH)_2$ or transient $Ca(OH)_2$ and the enhanced $CO_2$ molecular mobility at the carbonation stage [67,68].

Moreover, the $CO_2$ mineral carbonation of COFA doped with carbide slag was conducted in a pilot-scale circulating entrained-flow bed (CEB) rector (Figure 18). In a semi-dry atmosphere, the carbonation efficiency was enhanced 4 times higher than that of carbide-slag-doped COFA. It was mainly attributed to a thin liquid film formed on the surface of fly ash that facilitated $CO_2$ diffusion. At 550 °C, a maximal carbonation efficiency of 55% was obtained when adding 15% steam to the feed and injecting 6 kg/h of water into the rector system [69].

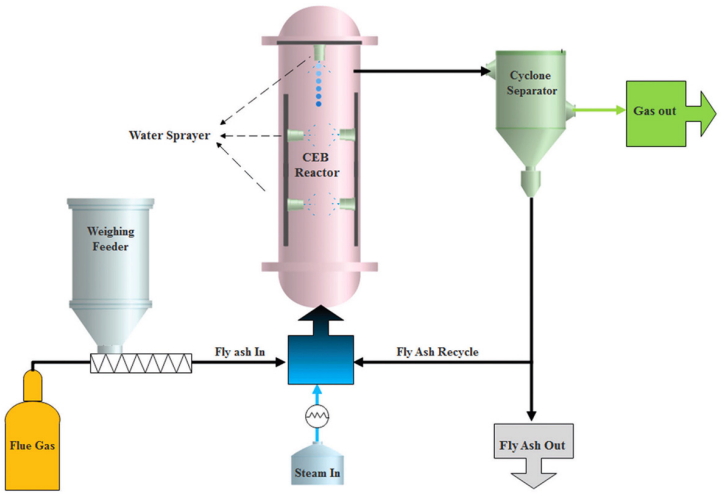


**Figure 18.** Diagram of the pilot-scale CEB bed reactor system for carbonation of fly ash [66]. Copyright 2018, with permission from Elsevier.

## 5. $CO_2$ Sequestration Materials Derived from COFA

Usually, COFA is rich in silica and alumina, which is beneficial to enhance the high-temperature $CO_2$ capture stability of CaO-based sorbents. Chen et al. [18,70] spared efforts to seeking a potentially effective approach to improve the capability of CaO-based sorbents mixed with COFA for $CO_2$ capture. The comparative studies on the effect of pretreatments (i.e., grinding, calcination, hydration, and leaching) of COFA on $CO_2$ capture performance of fly ash-modified CaO-based sorbents were conducted. The pretreatments of grinding and calcination for fly ash contributed to the improved $CO_2$ uptake capability for CaO-based sorbents. Acidic conditions were superior to basic conditions in enhancing $CO_2$ capture capacity and reactivity for CaO-based sorbents hydrated with fly ash [70]. The improved pore structure and the formation of inert stabilizers (i.e., $Ca_{12}Al_{14}O_{33}$ and $CaSiO_3$) within the CaO-based sorbents are the main reasons [71–73]. Particularly, the fly ash-modified sorbents with a mass ratio of slag/calcined calcium carbonate of 1:2, exhibited the $CO_2$ capture capacity of 0.19 g $CO_2$/g sorbent in the 30th cycle under severe calcination conditions, which was 3.8 times that of pure CaO [18].

Yan et al. [17] developed a green approach that involved silicon extraction from COFA by the method of alkali dissolution. Then, the synthetic nano silica was incorporated into CaO-based sorbents to improve both their cyclic $CO_2$ capacities and their sorption kinetics. Results exhibited that the synthetic nano silica-stabilized CaO-based sorbent still showed a higher $CO_2$ uptake of 0.2 g $CO_2$/g sorbent in short carbonation duration after 30 cycles (Figure 19), apparently increased by 155% over pure CaO. What was more important, the synthetic nano silica-stabilized CaO-based sorbent achieved approximately 90% of the total $CO_2$ uptake within ~20 s. The extremely fast $CO_2$ capture rate was very key for practical applications. The superior $CO_2$ capture performance of synthetic nano silica-stabilized sorbent was mainly ascribed to the evenly distributed $Ca_2SiO_4$, yielding a large amount of small pores directly exposed to $CO_2$ during cycles.

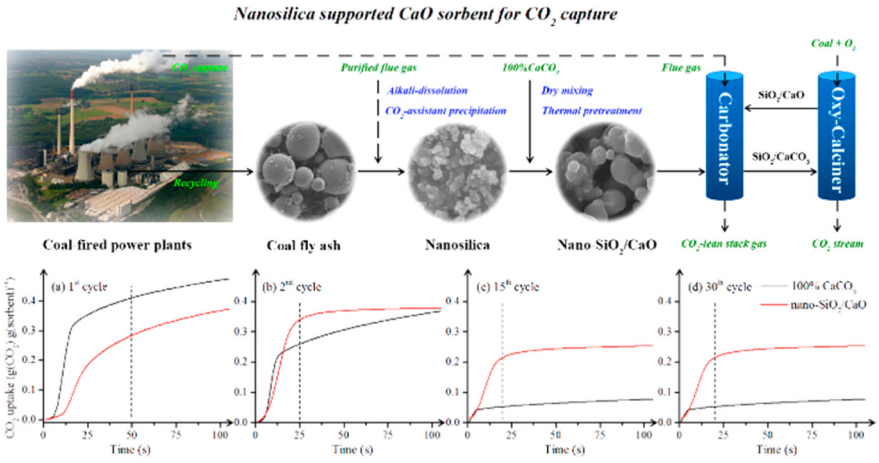


**Figure 19.** CaO sorbents doped with nano silica derived from COFA used for $CO_2$ capture [17]. Copyright 2017, with permission from the American Chemical Society.

The fly ash-stabilized, CaO-based sorbents were prepared via a physically dry-mixing method with different CaO precursors (i.e., CaO, $Ca(OH)_2$, $CaCO_3$, and $CaC_2O_4.H_2O$) [74]. After 30 cycles, the sorbent synthesized from $CaC_2O_4.H_2O$ (90 wt% of CaO in the sorbent) exhibited the highest $CO_2$ uptake of 0.38 g $CO_2$/g CaO. This sorbent still showed a desirable capacity of 0.27 g $CO_2$/g CaO even after being calcined at 920 °C in pure $CO_2$. The excellent performance of the fly ash-stabilized, CaO-based sorbents for cyclic $CO_2$ capture mainly resulted from the formation of highly dispersed inert $Ca_2Al_2SiO_7$ within the sorbent. Sreenivasulu et al. [75] further conducted the thermodynamic and kinetic studies of $CO_2$ capture using a COFA-doped sorbent (50 wt% CaO, 10 wt% MgO, and 40 wt% COFA). The thermodynamic studies confirmed both the feasibility of the reaction and the positive role

of COFA in improving $CO_2$ capture and reducing regeneration temperatures. They also proposed a model for both the reaction and diffusion kinetic control stages, which had been verified through the experimental data obtained. It was found that the rate constants of 2.5 and 0.8 $min^{-1}$ and activation energies of 23 and 30 kJ/mol were evaluated for reaction- and diffusion-controlled stages at 650 °C, respectively. The results clearly indicated the improved rate achieved by COFA-doped CaO-based sorbents along with their thermal stability.

Moreover, the $CO_2$ uptake capacity of hydrated lime mixed with fly ash under low-temperature and humid conditions was also investigated [76]. The reaction condition was set at 60 °C with 70% relative humidity. The fly ash-doped CaO-based sorbents containing <50 wt% of fly ash exhibited higher $CO_2$ uptake than hydrated lime without doping fly ash (~0.15 g $CO_2$/g sorbent). The sorbent doped with 30 wt% of fly ash showed a particularly high maximum $CO_2$ uptake of 0.26 g of $CO_2$/g sorbent. The enhanced microstructure resulting from the generation of calcium silicate hydrates was responsible for the improved reactivities of the fly ash-doped sorbents.

Moreover, various kinds of zeolites synthesized from COFAes were used to capture $CO_2$ in the flue gas. As shown in Figure 20, the typical octahedral prism and cube-shaped crystals were observed for the synthetic zeolites derived from COFAes, indicating the good generation of the desired zeolitic materials. Aquino et al. [77] comparatively measured the adsorption capacity of two synthetic zeolites (i.e., NaX and NaA types) from COFA and commercial zeolites and further assessed their performance in the temperature swing adsorption (TSA) testing process. It was found that NaX and NaA-type zeolites exhibited $CO_2$ adsorption capacities of 1.97 and 1.37 mmol $CO_2$/g adsorbent at 303 K, which were close to those of commercial zeolites. More importantly, the synthetic zeolites showed highly stable adsorption capacity during five cycles, demonstrating the possibility of practical application in TSA processes.

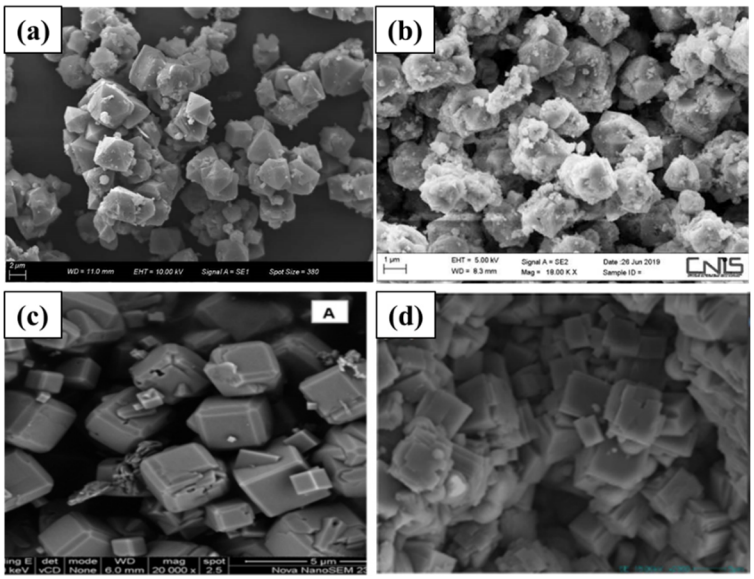


**Figure 20.** Micrographs of the zeolites synthesized from COFA (**a**) synthetic SZX, (**b**) PR1, (**c**) $NaA_{FA}$ and (**d**) HP1 zeolites. Modification from refs. [14,15,77,78].

Verrecchia et al. [14] focused on studying the effect of NaOH/COFA mass ratio, crystallization temperature, and duration on the synthesis of COFA-derived zeolites by the combined approach of fusion and hydrothermal. The major products contained NaX and amorphous compounds that were produced at 90 °C with a NaOH/COFA ratio of 1.2 for 7 h. They exhibited a capacity of 2.18 mol $CO_2$/kg adsorbent for $CO_2$ adsorption, accounting for 57% of the capacity of commercial 13X zeolites. Further, the central composite full factorial method was used to design experiments to optimize the synthesis parameters, aiming to improve the capacity of COFA-derived zeolites for $CO_2$ adsorption. It indicated that the

synthetic zeolite produced with the experimental conditions of 1.4 NaOH/COFA, 80 °C, and 7 h exhibited a markedly increased adsorption capacity of 3.3 mol $CO_2$/kg adsorbent (~86% of commercial 13X zeolites). Muriithi et al. [15] also successfully synthesized two types of zeolites (NaX and NaA type) from COFAes used for $CO_2$ capture. The synthetic NaX-type zeolite possessed hierarchical morphology with platy structures arranged in spherical clusters and exhibited desirable $CO_2$ physisorption properties.

Moreover, the collaborative activation method of microwave and ultrasound was adopted to synthesize K-MER zeolites with desirable crystallinity and high purity [78]. Comprehensively adjusting the crystallization duration, pressures, and dynamic pressure programs could produce K-MER zeolites exhibiting various morphologies. At 25 °C, the as-synthetic K-MER zeolites exhibited a maximal adsorption volume of $CO_2$ of 47.58 $cm^3$/g. The as-synthetic zeolites could also be used as catalysts to promote the cyanoethylatic reaction between methanol and acrylonitrile, which achieved a high acrylonitrile conversion rate of 99 wt% for 0.5 h under a pre-pressure of 1.5 MPa.

Furthermore, the COFA could be adopted as the raw material for producing synthetic hierarchical porous nano silica [16], nanoparticles MCM-41 [79], calcium silicate hydrate support [80], and silica-alumina aerogel [19] for $CO_2$ captured adsorbents. The hierarchical porous nano silica was mainly prepared through the collaborative method of microwave-assisted alkaline extraction and hydrothermal synthesis from fly ash derived from coal gasification [16]. The hierarchical porous nano silica had the isosteric adsorption heat of −30.06 kJ/mol, demonstrating that $CO_2$ adsorption involved both physisorption and chemisorption. The hierarchical porous nano silica exhibited a $CO_2$ adsorption capacity of 1.63 mmol $CO_2$/g adsorbent at 30 °C and 1 bar. The nanoparticle MCM-41 was functionalized with (3-aminopropyl) triethoxysilane and dispersed in diethylenetriamine (DETA) solution through ultrasonic dispersion method to prepare nanofluids for $CO_2$ capture [79]. The nanofluids coupled with high gravity technology markedly enhanced the $CO_2$ capture efficiency because of the improvement of grazing and hydrodynamic effect in a high gravity field (as shown in Figure 21), reaching ~95.7%. Qu et al. [80] synthesized highly porous COFA-derived calcium silicate hydrate (CSH) using the pore-expanded assistance of azeotropic distillation. The COFA-derived calcium silicate hydrate was then used as the support to prepare PEI@CSH adsorbents via impregnation. The 60% PEI@CSH-0.1 adsorbent exhibited the excellent $CO_2$ uptake of 198 mg $CO_2$/g adsorbent under ideal regeneration conditions, and after 10 cycles, the adsorption capacity remained at 103 mg $CO_2$/g adsorbent even under severe regeneration conditions.

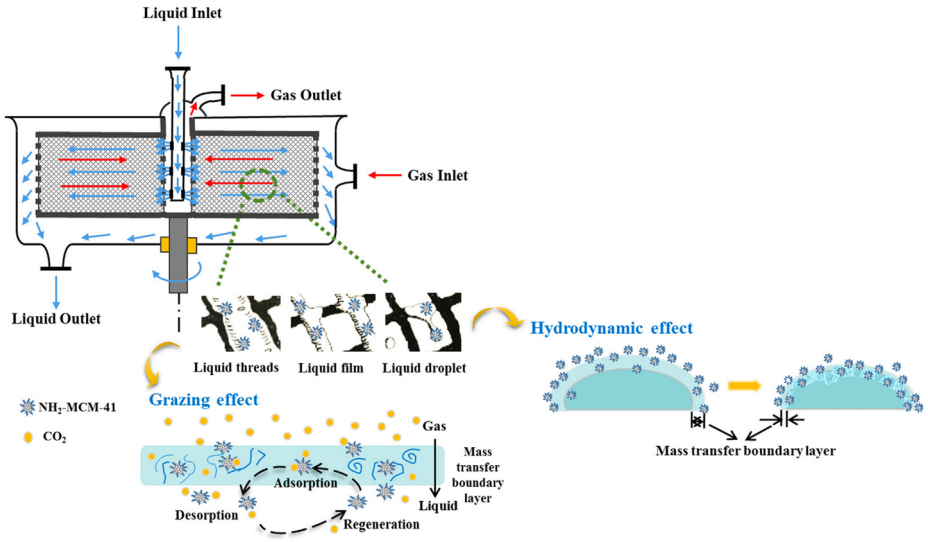


**Figure 21.** Mechanisms of $CO_2$ absorption improvement of nanofluids in high gravity rotating packed bed [79]. Copyright 2020, with permission from Elsevier.

The silica-alumina aerogel derived from COFA possessed good microstructure, which could also be used as the inert support to prepare $K_2CO_3$-based $CO_2$ adsorbent with a wetness impregnation method [19]. The synthetic silica-alumina aerogel support exhibited a relatively high specific surface area of 400 $m^2/g$ and a specific pore volume of 1.9 $cm^3/g$, and the proportion of mesopores within the support was over 99%. Therefore, the $K_2CO_3$-based adsorbent with $K_2CO_3$ load of 30 wt% achieved the maximal adsorption capacity of 2.02 mmol $CO_2/g$ adsorbent under the conditions of 60 °C, 15 vol% water vapor, and 15 vol% $CO_2$.

## 6. Conclusions and Prospects

This paper summarizes the $CO_2$ sequestration technologies using COFA reported in the literature. The relevant technical routes and representative research results from previous studies in this field are discussed and analyzed. The mineral $CO_2$ sequestration using COFA is one of the most promising technologies, which can be classified into direct and indirect carbonation. The direct $CO_2$ mineralization route is simple and highly practicable, which eliminates the extraction step of reactive components and minimizes the consumption of chemical reagents. Indirect $CO_2$ mineralization involves the extraction of reactive $Ca^{2+}$ from COFA with leaching agents (i.e., acid, ammonium salt, etc.) followed by carbonation reactions, which allow the production of high-value pure carbonates.

Moreover, the by-products derived from the $CO_2$ mineralization using COFA can be further utilized as feedstock to prepare composite gravel, cement mortar, geopolymers, mesoporous $\gamma$-$Al_2O_3$, and zeolite for toxic element trapping. The free CaO within COFA makes it possible to sequester $CO_2$ by dry process, and steam addition can effectively enhance carbonation efficiency. In addition, the silica and alumina contained in COFA can be used as materials for the synthesis of highly efficient $CO_2$ adsorbents. The COFA-modified CaO-based sorbents exhibit highly stable $CO_2$ capture performance due to the formation of extensive inert stabilizers, such as $Ca_{12}Al_{14}O_{33}$, $Ca_2Al_2SiO_7$, $CaSiO_3$, and $Ca_2SiO_4$. The $CO_2$ adsorption capability of the synthetic zeolites (i.e., NaX, NaA, and K-MER type) from coal fly ashes is comparable to that of commercial zeolites. Moreover, the nanoparticles MCM-41, calcium silicate hydrate, and silica-alumina aerogel derived from COFA can be used as the porous support of amine- or $K_2CO_3$-based adsorbents for low-temperature $CO_2$ capture.

The research on the development of $CO_2$ sequestration technologies using COFA in the past 10 years is summarized and analyzed. There are still some issues to be studied and solved.

(1) Although extensive research has been carried out to enhance the $CO_2$ mineralization performance of COFA, the current research is limited to the optimization of experimental parameters at the laboratory scale. In the future, this technology needs to be promoted for industry, which needs to consider the cost of various raw materials and energy consumption. Moreover, the carbon assets obtained from $CO_2$ fixation and the additional economic benefits of valued carbonation by-products also need to be considered. Therefore, it is urgent to achieve an integrated economic feasibility analysis or life cycle assessment concerning the industrial-scale $CO_2$ mineralization of COFA. The researchers can obtain the technical cost of $CO_2$ sequestration for direct and indirect carbonation of COFA via the above technical process economic analysis. This will be able to better demonstrate the practicality of the direct and indirect carbonation of COFA technology and the potential for industrial-scale promotion.

(2) COFA contains major associated elevated soluble trace elements (e.g., As, Cr, Mn, Cu, Sr, Ce, and V, etc.) that are potentially toxic to the biological system [63,81,82]. The heavy metal toxic elements are released into the surrounding environment (adversely affecting the plant and soil quality) by leaching of COFA once these are ponded or landfilled. Furthermore, these potentially toxic trace elements can reenter the food chain and human life cycle from these disposal sites via certain pathways [83]. Relevant scholars have investigated the accelerated carbonation of phosphogypsum [84]

and municipal solid waste incineration (MSWI) fly ash [21,81,85], and found that the carbonation reaction can solidify the heavy metal elements within waste to a certain extent in the realization of $CO_2$ sequestration. Hence, it is necessary to investigate the leaching characteristics of potentially toxic elements in COFA during the wet $CO_2$ mineralization process.

(3) For the synthesis of zeolites for $CO_2$ capture, the types of zeolite products are not rich enough. More technologies and processes should be developed to prepare low-cost and high-grade zeolites. Furthermore, the development of zeolites with highly selective adsorption and multi-effect functions should be the focus of research.

**Author Contributions:** Conceptualization, data curation, and writing—original draft preparation, L.J.; validation, formal analysis and visualization, L.C. and Y.Z.; supervision, G.L.; writing—review and editing, funding acquisition, J.S. All authors have read and agreed to the published version of the manuscript.

**Funding:** This research was funded by Jiangsu Education Department Fund (23KJB470025) and Graduate Research and Innovation Projects of Jiangsu Province (SJCX23_0605).

**Data Availability Statement:** The data presented in this study are available on request from the corresponding author.

**Conflicts of Interest:** The authors declare no conflict of interest.

## References

1. Wee, J.-H. A review on carbon dioxide capture and storage technology using coal fly ash. *Appl. Energy* **2013**, *106*, 143–151. [CrossRef]
2. Dindi, A.; Quang, D.V.; Vega, L.F.; Nashef, E.; Abu-Zahra, M.R. Applications of fly ash for $CO_2$ capture, utilization, and storage. *J. $CO_2$ Utilizat.* **2019**, *29*, 82–102. [CrossRef]
3. Wang, C.; Xu, G.; Gu, X.; Gao, Y.; Zhao, P. High value-added applications of coal fly ash in the form of porous materials: A review. *Ceram. Int.* **2021**, *47*, 22302–22315. [CrossRef]
4. Łach, M.; Grela, A.; Pławecka, K.; Guigou, M.D.; Mikuła, J.; Komar, N.; Bajda, T.; Korniejenko, K. Surface modification of synthetic zeolites with Ca and HDTMA compounds with determination of their phytoavailability and comparison of CEC and AEC parameters. *Materials* **2022**, *15*, 4083. [CrossRef]
5. Wang, J.; Yang, Y.; Jia, Q.; Shi, Y.; Guan, Q.; Yang, N.; Wang, Q.; Ning, P. A critical review on solid waste derived $CO_2$ capturing materials. *ChemSusChem* **2019**, *15*, 4083.
6. Sun, J.; Liang, C.; Tong, X.; Guo, Y.; Li, W.; Zhao, C.; Zhang, J.; Lu, P. Evaluation of high-temperature $CO_2$ capture performance of cellulose-templated CaO-based pellets. *Fuel* **2019**, *239*, 1046–1054. [CrossRef]
7. Sheng, C.; Li, Y. Experimental study of ash formation during pulverized coal combustion in $O_2/CO_2$ mixtures. *Fuel* **2008**, *87*, 1297–1305. [CrossRef]
8. Xu, M.; Yu, D.; Yao, H.; Liu, X.; Qiao, Y. Coal combustion-generated aerosols: Formation and properties. *Proc. Combust. Inst.* **2011**, *33*, 1681–1697. [CrossRef]
9. Uliasz-Bocheńczyk, A.; Pawluk, A.; Pyzalski, M. The mineral sequestration of $CO_2$ with the use of fly ash from the co-combustion of coal and biomass. *Gospod. Surowc. Mineral.* **2017**, *33*, 143–155. [CrossRef]
10. Jia, B.; Tsau, J.-S.; Barati, R. A review of the current progress of $CO_2$ injection EOR and carbon storage in shale oil reservoirs. *Fuel* **2019**, *236*, 404–427. [CrossRef]
11. Jia, B.; Xian, C.; Tsau, J.-S.; Zuo, X.; Jia, W. Status and outlook of oil field chemistry-assisted analysis during the energy transition period. *Energ. Fuel* **2022**, *36*, 12917–12945. [CrossRef]
12. Bui, M.; Adjiman, C.S.; Bardow, A.; Anthony, E.J.; Boston, A.; Brown, S.; Fennell, P.S.; Fuss, S.; Galindo, A.; Hackett, L.A. Carbon capture and storage (CCS): The way forward. *Energy Environ. Sci.* **2018**, *11*, 1062–1176. [CrossRef]
13. Bobicki, E.R.; Liu, Q.; Xu, Z.; Zeng, H. Carbon capture and storage using alkaline industrial wastes. *Prog. Energy Combust.* **2012**, *38*, 302–320. [CrossRef]
14. Verrecchia, G.; Cafiero, L.; de Caprariis, B.; Dell'Era, A.; Pettiti, I.; Tuffi, R.; Scarsella, M. Study of the parameters of zeolites synthesis from coal fly ash in order to optimize their $CO_2$ adsorption. *Fuel* **2020**, *276*, 118041. [CrossRef]
15. Muriithi, G.N.; Petrik, L.F.; Doucet, F.J. Synthesis, characterisation and $CO_2$ adsorption potential of NaA and NaX zeolites and hydrotalcite obtained from the same coal fly ash. *J. $CO_2$ Utilizat.* **2020**, *36*, 220–230. [CrossRef]
16. Liu, Y.; Wang, Z.; Zhao, W.; Hou, J.; Cui, L.; Zou, L.; Li, C.; Li, H.; Wu, Y.; Xu, R. Hierarchical porous nanosilica derived from coal gasification fly ash with excellent $CO_2$ adsorption performance. *Chem. Eng. J.* **2023**, *455*, 140622. [CrossRef]
17. Yan, F.; Jiang, J.; Li, K.; Liu, N.; Chen, X.; Gao, Y.; Tian, S. Green synthesis of nanosilica from coal fly ash and its stabilizing effect on CaO sorbents for $CO_2$ capture. *Environ. Sci. Technol.* **2017**, *51*, 7606–7615. [CrossRef]

18. Chen, H.; Khalili, N. Fly-ash-modified calcium-based sorbents tailored to $CO_2$ capture. *Ind. Eng. Chem. Res.* **2017**, *56*, 1888–1894. [CrossRef]
19. Guo, B.; Zhang, J.; Wang, Y.; Qiao, X.; Xiang, J.; Jin, Y. Study on $CO_2$ adsorption capacity and kinetic mechanism of $CO_2$ adsorbent prepared from fly ash. *Energy* **2023**, *263*, 125764. [CrossRef]
20. Shao, X.; Qin, B.; Shi, Q.; Yang, Y.; Ma, Z.; Xu, Y.; Hao, M.; Jiang, Z.; Jiang, W. Study on the sequestration capacity of fly ash on $CO_2$ and employing the product to prevent spontaneous combustion of coal. *Fuel* **2023**, *334*, 126378. [CrossRef]
21. Bertos, M.F.; Li, X.; Simons, S.; Hills, C.; Carey, P. Investigation of accelerated carbonation for the stabilisation of MSW incinerator ashes and the sequestration of $CO_2$. *Green Chem.* **2004**, *6*, 428–436. [CrossRef]
22. Muriithi, G.N.; Petrik, L.F.; Fatoba, O.; Gitari, W.M.; Doucet, F.J.; Nel, J.; Nyale, S.M.; Chuks, P.E. Comparison of $CO_2$ capture by ex-situ accelerated carbonation and in in-situ naturally weathered coal fly ash. *J. Environ. Manag.* **2013**, *127*, 212–220. [CrossRef]
23. Ji, L.; Yu, H.; Zhang, R.; French, D.; Grigore, M.; Yu, B.; Wang, X.; Yu, J.; Zhao, S. Effects of fly ash properties on carbonation efficiency in $CO_2$ mineralisation. *Fuel Process. Technol.* **2019**, *188*, 79–88. [CrossRef]
24. Yuan, Q.; Yang, G.; Zhang, Y.; Wang, T.; Wang, J.; Romero, C.E. Supercritical $CO_2$ coupled with mechanical force to enhance carbonation of fly ash and heavy metal solidification. *Fuel* **2022**, *315*, 123154. [CrossRef]
25. Yuan, Q.; Zhang, Y.; Wang, T.; Wang, J.; Romero, C.E. Mineralization characteristics of coal fly ash in the transition from non-supercritical $CO_2$ to supercritical $CO_2$. *Fuel* **2022**, *318*, 123636. [CrossRef]
26. Baciocchi, R.; Costa, G.; Lategano, E.; Marini, C.; Polettini, A.; Pomi, R.; Postorino, P.; Rocca, S. Accelerated carbonation of different size fractions of bottom ash from RDF incineration. *Waste Manag.* **2010**, *30*, 1310–1317. [CrossRef] [PubMed]
27. Shih, S.-M.; Lin, J.-P.; Shiau, G.-Y. Dissolution rates of limestones of different sources. *J. Hazard. Mater.* **2000**, *79*, 159–171. [CrossRef] [PubMed]
28. Sanchez, F.; Gervais, C.; Garrabrants, A.; Barna, R.; Kosson, D. Leaching of inorganic contaminants from cement-based waste materials as a result of carbonation during intermittent wetting. *Waste Manag.* **2002**, *22*, 249–260. [CrossRef] [PubMed]
29. Siriwardena, D.P.; Peethamparan, S. Quantification of $CO_2$ sequestration capacity and carbonation rate of alkaline industrial byproducts. *Constr. Build. Mater.* **2015**, *91*, 216–224. [CrossRef]
30. Back, M.; Kuehn, M.; Stanjek, H.; Peiffer, S. Reactivity of alkaline lignite fly ashes towards $CO_2$ in water. *Environ. Sci. Technol.* **2008**, *42*, 4520–4526. [CrossRef]
31. La Plante, E.C.; Mehdipour, I.; Shortt, I.; Yang, K.; Simonetti, D.; Bauchy, M.; Sant, G.N. Controls on $CO_2$ mineralization using natural and industrial alkaline solids under ambient conditions. *ACS Sustain. Chem. Eng.* **2021**, *9*, 10727–10739. [CrossRef]
32. Pan, S.-Y.; Hung, C.-H.; Chan, Y.-W.; Kim, H.; Li, P.; Chiang, P.-C. Integrated $CO_2$ fixation, waste stabilization, and product utilization via high-gravity carbonation process exemplified by circular fluidized bed fly ash. *ACS Sustain. Chem. Eng.* **2016**, *4*, 3045–3052. [CrossRef]
33. Revathy, T.D.R.; Ramachandran, A.; Palanivelu, K. Carbon capture and storage using coal fly ash with flue gas. *Clean Technol. Environ. Policy* **2021**, *24*, 1053–1071. [CrossRef]
34. Ukwattage, N.; Ranjith, P.; Wang, S. Investigation of the potential of coal combustion fly ash for mineral sequestration of $CO_2$ by accelerated carbonation. *Energy* **2013**, *52*, 230–236. [CrossRef]
35. Miao, E.; Du, Y.; Zheng, X.; Zhang, X.; Xiong, Z.; Zhao, Y.; Zhang, J. Kinetic analysis on $CO_2$ sequestration from flue gas through direct aqueous mineral carbonation of circulating fluidized bed combustion fly ash. *Fuel* **2023**, *342*, 127851. [CrossRef]
36. Montes-Hernandez, G.; Perez-Lopez, R.; Renard, F.; Nieto, J.; Charlet, L. Mineral sequestration of $CO_2$ by aqueous carbonation of coal combustion fly-ash. *J. Hazard. Mater.* **2009**, *161*, 1347–1354. [CrossRef]
37. Bauer, M.; Gassen, N.; Stanjek, H.; Peiffer, S. Carbonation of lignite fly ash at ambient T and P in a semi-dry reaction system for $CO_2$ sequestration. *Appl. Geochem.* **2011**, *26*, 1502–1512. [CrossRef]
38. Ukwattage, N.L.; Ranjith, P.; Yellishetty, M.; Bui, H.H.; Xu, T. A laboratory-scale study of the aqueous mineral carbonation of coal fly ash for $CO_2$ sequestration. *J. Clean. Prod.* **2015**, *103*, 665–674. [CrossRef]
39. Dananjayan, R.R.T.; Kandasamy, P.; Andimuthu, R. Direct mineral carbonation of coal fly ash for $CO_2$ sequestration. *J. Clean. Prod.* **2016**, *112*, 4173–4182. [CrossRef]
40. Patel, A.; Basu, P.; Acharya, B. An investigation into partial capture of $CO_2$ released from a large coal/petcoke fired circulating fluidized bed boiler with limestone injection using its fly and bottom ash. *J. Environ. Chem. Eng.* **2017**, *5*, 667–678. [CrossRef]
41. Ho, H.-J.; Iizuka, A.; Shibata, E. Utilization of low-calcium fly ash via direct aqueous carbonation with a low-energy input: Determination of carbonation reaction and evaluation of the potential for $CO_2$ sequestration and utilization. *J. Environ. Manag.* **2021**, *288*, 112411. [CrossRef] [PubMed]
42. Ji, L.; Yu, H.; Wang, X.; Grigore, M.; French, D.; Gözükara, Y.M.; Yu, J.; Zeng, M. $CO_2$ sequestration by direct mineralisation using fly ash from Chinese Shenfu coal. *Fuel Process. Technol.* **2017**, *156*, 429–437. [CrossRef]
43. Jo, H.Y.; Ahn, J.-H.; Jo, H. Evaluation of the $CO_2$ sequestration capacity for coal fly ash using a flow-through column reactor under ambient conditions. *J. Hazard. Mater.* **2012**, *241*, 127–136. [CrossRef]
44. Ji, L.; Zheng, X.; Zhang, L.; Feng, L.; Li, K.; Yu, H.; Yan, S. Feasibility and mechanism of an amine-looping process for efficient $CO_2$ mineralization using alkaline ashes. *Chem. Eng. J.* **2022**, *430*, 133118. [CrossRef]
45. Ji, L.; Yu, H.; Li, K.; Yu, B.; Grigore, M.; Yang, Q.; Wang, X.; Chen, Z.; Zeng, M.; Zhao, S. Integrated absorption-mineralisation for low-energy $CO_2$ capture and sequestration. *Appl. Energy* **2018**, *225*, 356–366. [CrossRef]

46. Nyambura, M.G.; Mugera, G.W.; Felicia, P.L.; Gathura, N.P. Carbonation of brine impacted fractionated coal fly ash: Implications for $CO_2$ sequestration. *J. Environ. Manag.* **2011**, *92*, 655–664. [CrossRef]
47. Hosseini, T.; Selomulya, C.; Haque, N.; Zhang, L. Indirect carbonation of victorian brown coal fly ash for $CO_2$ sequestration: Multiple-cycle leaching-carbonation and magnesium leaching kinetic modeling. *Energy Fuel* **2014**, *28*, 6481–6493. [CrossRef]
48. He, L.L.; Yu, D.X.; Lv, W.Z.; Wu, J.Q.; Xu, M.H. *$CO_2$ Sequestration by Indirect Carbonation of High-Calcium Coal Fly Ash*; Advanced Materials Research, Trans Tech Publications: Geneva, Switzerland, 2013; pp. 2870–2874.
49. He, L.; Yu, D.; Lv, W.; Wu, J.; Xu, M. A novel method for $CO_2$ sequestration via indirect carbonation of coal fly ash. *Ind. Eng. Chem. Res.* **2013**, *52*, 15138–15145. [CrossRef]
50. Jo, H.Y.; Kim, J.H.; Lee, Y.J.; Lee, M.; Choh, S.-J. Evaluation of factors affecting mineral carbonation of $CO_2$ using coal fly ash in aqueous solutions under ambient conditions. *Chem. Eng. J.* **2012**, *183*, 77–87. [CrossRef]
51. Sun, Y.; Parikh, V.; Zhang, L. Sequestration of carbon dioxide by indirect mineralization using Victorian brown coal fly ash. *J. Hazard. Mater.* **2012**, *209*, 458–466. [CrossRef]
52. Ho, H.-J.; Iizuka, A.; Shibata, E.; Ojumu, T. Circular indirect carbonation of coal fly ash for carbon dioxide capture and utilization. *J. Environ. Chem. Eng.* **2022**, *10*, 108269. [CrossRef]
53. Lu, L.; Fang, Y.; Huang, Z.; Huang, Y.; Ren, Z.J. Self-sustaining carbon capture and mineralization via electrolytic carbonation of coal fly ash. *Chem. Eng. J.* **2016**, *306*, 330–335. [CrossRef]
54. Huang, Y.; Zheng, X.; Wei, Y.; He, Q.; Yan, S.; Ji, L. Protonated amines mediated $CO_2$ mineralization of coal fly ash and polymorph selection of $CaCO_3$. *Chem. Eng. J.* **2022**, *450*, 138121. [CrossRef]
55. Zheng, X.; Liu, J.; Wang, Y.; Wang, Y.; Ji, L.; Yan, S. Regenerable glycine induces selective preparation of vaterite $CaCO_3$ by calcium leaching and $CO_2$ mineralization from coal fly ash. *Chem. Eng. J.* **2023**, *459*, 141536. [CrossRef]
56. Zheng, X.; Liu, J.; Wei, Y.; Li, K.; Yu, H.; Wang, X.; Ji, L.; Yan, S. Glycine-mediated leaching-mineralization cycle for $CO_2$ sequestration and $CaCO_3$ production from coal fly ash: Dual functions of glycine as a proton donor and receptor. *Chem. Eng. J.* **2022**, *440*, 135900. [CrossRef]
57. Ragipani, R.; Sreenivasan, K.; Anex, R.P.; Zhai, H.; Wang, B. Direct Air Capture and Sequestration of $CO_2$ by Accelerated Indirect Aqueous Mineral Carbonation under Ambient Conditions. *ACS Sustain. Chem. Eng.* **2022**, *10*, 7852–7861. [CrossRef]
58. Ren, K.; Ma, S.; Feng, Y.; Xu, N.; Bai, S. Study on the composite gravel preparation and the synergistic absorption of $CO_2$ by fly ash of CFB boiler. *Fuel* **2023**, *342*, 127843. [CrossRef]
59. Siriruang, C.; Toochinda, P.; Julnipitawong, P.; Tangtermsirikul, S. $CO_2$ capture using fly ash from coal fired power plant and applications of $CO_2$-captured fly ash as a mineral admixture for concrete. *J. Environ. Manag.* **2016**, *170*, 70–78. [CrossRef]
60. Chen, T.; Bai, M.; Gao, X. Carbonation curing of cement mortars incorporating carbonated fly ash for performance improvement and $CO_2$ sequestration. *J. $CO_2$ Utilizat.* **2021**, *51*, 101633. [CrossRef]
61. Freire, A.L.; Moura-Nickel, C.D.; Scaratti, G.; De Rossi, A.; Araújo, M.H.; Júnior, A.D.N.; Rodrigues, A.E.; Castellón, E.R.; Moreira, R.d.F.P.M. Geopolymers produced with fly ash and rice husk ash applied to $CO_2$ capture. *J. Clean. Prod.* **2020**, *273*, 122917. [CrossRef]
62. Yin, T.; Yin, S.; Srivastava, A.; Gadikota, G. Regenerable solvents mediate accelerated low temperature $CO_2$ capture and carbon mineralization of ash and nano-scale calcium carbonate formation. *Resour. Conservat. Recycl.* **2022**, *180*, 106209. [CrossRef]
63. Monasterio-Guillot, L.; Alvarez-Lloret, P.; Ibañez-Velasco, A.; Fernandez-Martinez, A.; Ruiz-Agudo, E.; Rodriguez-Navarro, C. $CO_2$ sequestration and simultaneous zeolite production by carbonation of coal fly ash: Impact on the trapping of toxic elements. *J. $CO_2$ Utilizat.* **2020**, *40*, 101263. [CrossRef]
64. Yan, F.; Jiang, J.; Liu, N.; Gao, Y.; Meng, Y.; Li, K.; Chen, X. Green synthesis of mesoporous $\gamma$-$Al_2O_3$ from coal fly ash with simultaneous on-site utilization of $CO_2$. *J. Hazard. Mater.* **2018**, *359*, 535–543. [CrossRef]
65. Liu, W.; Su, S.; Xu, K.; Chen, Q.; Xu, J.; Sun, Z.; Wang, Y.; Hu, S.; Wang, X.; Xue, Y. $CO_2$ sequestration by direct gas–solid carbonation of fly ash with steam addition. *J. Clean. Prod.* **2018**, *178*, 98–107. [CrossRef]
66. Ćwik, A.; Casanova, I.; Rausis, K.; Koukouzas, N.; Zarębska, K. Carbonation of high-calcium fly ashes and its potential for carbon dioxide removal in coal fired power plants. *J. Clean. Prod.* **2018**, *202*, 1026–1034. [CrossRef]
67. Blamey, J.; Manovic, V.; Anthony, E.J.; Dugwell, D.R.; Fennell, P.S. On steam hydration of CaO-based sorbent cycled for $CO_2$ capture. *Fuel* **2015**, *150*, 269–277. [CrossRef]
68. González, B.; Liu, W.; Sultan, D.; Dennis, J. The effect of steam on a synthetic Ca-based sorbent for carbon capture. *Chem. Eng. J.* **2016**, *285*, 378–383. [CrossRef]
69. Liu, R.; Wang, X.; Gao, S. $CO_2$ capture and mineralization using carbide slag doped fly ash. *Greenhouse Gases Sci. Technol.* **2020**, *10*, 103–115. [CrossRef]
70. Chen, H.; Wang, F.; Zhao, C.; Khalili, N. The effect of fly ash on reactivity of calcium based sorbents for $CO_2$ capture. *Chem. Eng. J.* **2017**, *309*, 725–737. [CrossRef]
71. Ma, X.; Li, Y.; Yan, X.; Zhang, W.; Zhao, J.; Wang, Z. Preparation of a morph-genetic CaO-based sorbent using paper fibre as a biotemplate for enhanced $CO_2$ capture. *Chem. Eng. J.* **2019**, *361*, 235–244. [CrossRef]
72. Li, Y.; Zhao, C.; Ren, Q.; Duan, L.; Chen, H.; Chen, X. Effect of rice husk ash addition on $CO_2$ capture behavior of calcium-based sorbent during calcium looping cycle. *Fuel Process. Technol.* **2009**, *90*, 825–834. [CrossRef]
73. Liu, Y.; Yang, X.; Zhao, L.; Lei, F.; Xiao, Y. Effects of steam on $CO_2$ absorption ability of calcium-based sorbent modified by peanut husk ash. *Sci. China Technol. Sci.* **2017**, *60*, 953–962. [CrossRef]

74. Yan, F.; Jiang, J.; Li, K.; Tian, S.; Zhao, M.; Chen, X. Performance of Coal Fly Ash Stabilized, CaO-based Sorbents under Different Carbonation–Calcination Conditions. *ACS Sustain. Chem. Eng.* **2015**, *3*, 2092–2099. [CrossRef]
75. Sreenivasulu, B.; Sreedhar, I.; Venugopal, A.; Reddy, B.; Raghavan, K. Thermokinetic investigations of high temperature carbon capture using a coal fly ash doped sorbent. *Energy Fuel* **2017**, *31*, 6320–6328. [CrossRef]
76. Liu, C.-F.; Yang, C.-H.; Shih, S.-M. $CO_2$ Capture by Fly Ash/Hydrated Lime Sorbents at Low Temperatures. *Ind. Eng. Chem. Res.* **2022**, *61*, 4774–4783. [CrossRef]
77. De Aquino, T.F.; Estevam, S.T.; Viola, V.O.; Marques, C.R.; Zancan, F.L.; Vasconcelos, L.B.; Riella, H.G.; Pires, M.J.; Morales-Ospino, R.; Torres, A.E.B. $CO_2$ adsorption capacity of zeolites synthesized from coal fly ashes. *Fuel* **2020**, *276*, 118143. [CrossRef]
78. Chen, W.; Song, G.; Lin, Y.; Qiao, J.; Wu, T.; Yi, X.; Kawi, S. A green and efficient strategy for utilizing of coal fly ash to synthesize K-MER zeolite as catalyst for cyanoethylation and adsorbent of $CO_2$. *Micropor. Mesopor. Mater.* **2021**, *326*, 111353. [CrossRef]
79. Cheng, S.-Y.; Liu, Y.-Z.; Qi, G.-S. Experimental study of $CO_2$ capture enhanced by coal fly ash-synthesized $NH_2$-MCM-41 coupled with high gravity technology. *Chem. Eng. J.* **2020**, *400*, 125946. [CrossRef]
80. Qu, F.; Yan, F.; Shen, X.; Li, C.; Chen, H.; Wang, P.; Zhang, Z. Novel PEI@ CSH adsorbents derived from coal fly ash enabling efficient and in-situ $CO_2$ capture: The anti-urea mechanism of CSH support. *J. Clean. Prod.* **2022**, *378*, 134420. [CrossRef]
81. Chen, T.-L.; Chen, Y.-H.; Dai, M.-Y.; Chiang, P.-C. Stabilization-solidification-utilization of MSWI fly ash coupling $CO_2$ mineralization using a high-gravity rotating packed bed. *Waste Manag.* **2021**, *121*, 412–421. [CrossRef]
82. Fernandez-Turiel, J.; De Carvalho, W.; Cabañas, M.; Querol, X.; Lopez-Soler, A. Mobility of heavy metals from coal fly ash. *Environ. Geol.* **1994**, *23*, 264–270. [CrossRef]
83. Koukouzas, N.; Ketikidis, C.; Itskos, G. Heavy metal characterization of CFB-derived coal fly ash. *Fuel Process. Technol* **2011**, *92*, 441–446. [CrossRef]
84. Cardenas-Escudero, C.; Morales-Flórez, V.; Pérez-López, R.; Santos, A.; Esquivias, L. Procedure to use phosphogypsum industrial waste for mineral $CO_2$ sequestration. *J. Hazard. Mater.* **2011**, *196*, 431–435. [CrossRef]
85. Chen, J.; Fu, C.; Mao, T.; Shen, Y.; Li, M.; Lin, X.; Li, X.; Yan, J. Study on the accelerated carbonation of MSWI fly ash under ultrasonic excitation: $CO_2$ capture, heavy metals solidification, mechanism and geochemical modelling. *Chem. Eng. J.* **2022**, *450*, 138418. [CrossRef]